PROCEEDINGS A

royalsocietypublishing.org/journal/rspa

Research

Check for updates

Cite this article: Xiao D, Prior CB, Yeates AR. 2025 Winding and magnetic helicity in periodic domains. *Proc. R. Soc. A* **481**: 20240152.
https://doi.org/10.1098/rspa.2024.0152

Received: 26 February 2024
Accepted: 29 November 2024

Subject Category:
Mathematics

Subject Areas:
mathematical physics, fluid mechanics, astrophysics

Keywords:
magnetohydrodynamics, magnetic topology, magnetic helicity, winding number, periodic domains

Author for correspondence:
Daining Xiao
e-mail: dx216@cantab.ac.uk

Winding and magnetic helicity in periodic domains

Daining Xiao[1,2], Christopher B. Prior[1] and Anthony R. Yeates[1]

[1]Department of Mathematical Sciences, University of Durham, Durham DH1 3LE, UK
[2]School of Mathematics and Statistics, University of Glasgow, Glasgow G12 8QQ, UK

DX, 0000-0001-9027-3245

In simply connected Euclidean domains, it is well known that the topological complexity of a given magnetic field can be quantified by its magnetic helicity, which is equivalent to the total, flux-weighted winding number of magnetic field lines. Often considered in analytical and numerical studies are domains periodic in two lateral dimensions (periodic domains) that are multiply connected and homoeomorphic to a 2-torus. Whether this equivalence can be generalized to periodic domains remains an open question, first posed by Berger (Berger 1996 *J. Geophys. Res.* **102**, 2637–2644 (doi:10.1029/96JA01896)). In this article, we answer in the affirmative by defining the novel periodic winding of curves and identifying a vector potential that recovers the topological interpretation of magnetic helicity as winding. Key properties of the topologically defined magnetic helicity in periodic domains are also proved, including its time-conservation in ideal magnetohydrodynamical flows, its connection to Fourier approaches and its relationship to gauge transformations.

1. Introduction

Let $V \subset \mathbb{R}^3$ be a simply connected domain with smooth (possibly empty) boundary ∂V and outward unit normal $\hat{\boldsymbol{n}}$. Poincaré Lemma implies that any smooth (assumed hereafter for all functions) divergence-free vector field $\boldsymbol{B}$, which shall be called a *magnetic field*, can be written as $\boldsymbol{B} = \nabla \times \boldsymbol{A}$ for some *vector potential* $\boldsymbol{A}$. In the case when V is *magnetically closed*, i.e. $\boldsymbol{B} \cdot \hat{\boldsymbol{n}}|_{\partial V} = 0$, it was first proved by Woltjer [1] that the integral

THE ROYAL SOCIETY PUBLISHING

$$H(\boldsymbol{B}) \equiv \int_V \boldsymbol{A}\cdot\boldsymbol{B}\,\mathrm{d}V, \tag{1.1}$$

called *(magnetic) helicity*, is invariant under ideal magnetohydrodynamical evolution. Moreau [2] established an analogous conservation law in ideal hydrodynamics by replacing $\boldsymbol{A}$ by flow velocity $\boldsymbol{u}$ and $\boldsymbol{B}$ by vorticity $\nabla\times\boldsymbol{u}$. Geometrically, the magnetic closedness of V implies that the integral curves of $\boldsymbol{B}$ (or magnetic field lines; hereafter '$\boldsymbol{B}$-lines') never intersect ∂V transversally. With this assumption, Moffatt [3] and Arnold [4] showed that $H(\boldsymbol{B})$ is equivalent to the total, flux-weighted *(Gauss) linking number* of $\boldsymbol{B}$-lines (see also Moffatt & Ricca [5]),

$$H(\boldsymbol{B}) = \frac{1}{4\pi}\int_V\int_V \boldsymbol{B}(\boldsymbol{x})\cdot\boldsymbol{B}(\boldsymbol{x}')\times\frac{\boldsymbol{x}-\boldsymbol{x}'}{|\boldsymbol{x}-\boldsymbol{x}'|^3}\,\mathrm{d}^3\boldsymbol{x}'\,\mathrm{d}^3\boldsymbol{x}, \tag{1.2}$$

a double integral over all pairs of distinct points $\boldsymbol{x},\boldsymbol{x}'\in V$. This result bridges helicity to the entanglement of $\boldsymbol{B}$-lines, which quantifies the topological complexity of the magnetic field.

By contrast, when V is *magnetically open*, meaning that $\boldsymbol{B}\cdot\hat{\boldsymbol{n}}|_{\partial V}\neq 0$ or $\boldsymbol{B}$-lines transversally intersect ∂V, the above relation (1.2) becomes invalid as the Biot–Savart law used to derive it fails to produce a vector potential [6]. Another, perhaps better known, issue associated with helicity in magnetically open domains is the non-uniqueness of vector potentials. Given any scalar field χ, the *gauge transformation* $\boldsymbol{A}\mapsto\boldsymbol{A}'\equiv\boldsymbol{A}+\nabla\chi$ yields another permissible vector potential $\boldsymbol{A}'$ for $\boldsymbol{B}$ while changing $H(\boldsymbol{B})$, as defined in (1.1), by a boundary integral

$$H(\boldsymbol{B}) \mapsto H(\boldsymbol{B}) + \int_{\partial V}\chi\boldsymbol{B}\cdot\hat{\boldsymbol{n}}\,\mathrm{d}A. \tag{1.3}$$

One common alternative to (1.1) is the *relative helicity*, $H(\boldsymbol{B};\boldsymbol{B}_{\mathrm{ref}})$, introduced in Berger & Field [7], which can be defined by the Finn–Antonsen formula [8]:

$$H(\boldsymbol{B};\boldsymbol{B}_{\mathrm{ref}}) \equiv \int_V (\boldsymbol{A}+\boldsymbol{A}_{\mathrm{ref}})\cdot(\boldsymbol{B}-\boldsymbol{B}_{\mathrm{ref}})\,\mathrm{d}V. \tag{1.4}$$

Here, $\boldsymbol{B}_{\mathrm{ref}}$ is a *reference magnetic field* that satisfies $(\boldsymbol{B}-\boldsymbol{B}_{\mathrm{ref}})\cdot\hat{\boldsymbol{n}}|_{\partial V}=0$, and $\boldsymbol{A},\boldsymbol{A}_{\mathrm{ref}}$ are the respective vector potentials for $\boldsymbol{B}$, $\boldsymbol{B}_{\mathrm{ref}}$. While (1.4) is invariant under gauge transformations of $\boldsymbol{A}$ and $\boldsymbol{A}_{\mathrm{ref}}$, the value of $H(\boldsymbol{B};\boldsymbol{B}_{\mathrm{ref}})$ can still be arbitrary due to the freedom in choosing $\boldsymbol{B}_{\mathrm{ref}}$ as shown in [9]. Usually, $\boldsymbol{B}_{\mathrm{ref}}$ is taken to be the unique potential field $\boldsymbol{B}_p$ with $\nabla\times\boldsymbol{B}_p=\boldsymbol{0}$ and matching boundary conditions (e.g. [10] for a review). Moreover, there is a lack of explicit topological interpretation for (1.4) in terms of $\boldsymbol{B}$-lines that is analogous to (1.2).

In magnetically open Euclidean domains of the form $V_{\mathrm{E}}\equiv\mathbb{R}^2\times[0,1]$, Berger [12] first proposed a topological interpretation of relative helicity by making a special choice of $\boldsymbol{B}_{\mathrm{ref}}$. This is reproduced in Prior & Yeates [9] by identifying a special vector potential $\boldsymbol{A}^{\mathrm{W}}$ and substituting into the original definition (1.1), yielding *(Euclidean) winding helicity*

$$H^{\mathrm{W}}(\boldsymbol{B}) \equiv \int_{V_{\mathrm{E}}}\boldsymbol{A}^{\mathrm{W}}\cdot\boldsymbol{B}\,\mathrm{d}V. \tag{1.5}$$

Here, the *winding gauge* $\boldsymbol{A}^{\mathrm{W}}$ is defined to satisfy

$$\nabla_S\cdot\boldsymbol{A}^{\mathrm{W}}=0, \quad \text{where} \quad \nabla_S\equiv(\partial_x,\partial_y,0), \tag{1.6}$$

on each horizontal plane $S_w\equiv\mathbb{R}^2\times\{w\}$ with coordinates (x,y) and labelled by vertical coordinate $w\in[0,1]$. In both accounts, $H^{\mathrm{W}}(\boldsymbol{B})$ can be written as the total, flux-weighted winding number of $\boldsymbol{B}$-lines, i.e.

$$H^{\mathrm{W}}(\boldsymbol{B}) = \frac{1}{2\pi}\int_0^1\int_{S_w}\int_{S_w}\boldsymbol{B}(\boldsymbol{x})\cdot\boldsymbol{B}(\boldsymbol{x}')\times\frac{\boldsymbol{x}-\boldsymbol{x}'}{|\boldsymbol{x}-\boldsymbol{x}'|^2}\,\mathrm{d}^2\boldsymbol{x}'\,\mathrm{d}^2\boldsymbol{x}\,\mathrm{d}w, \tag{1.7}$$

analogous to (1.2); see also Prior & MacTaggart [13]. For magnetically closed domains, it is clear that (1.7) must reduce to the flux-weighted Gauss linking integral (1.2) by gauge invariance.

royalsocietypublishing.org/journal/rspa *Proc. R. Soc. A* **481:** 20240152

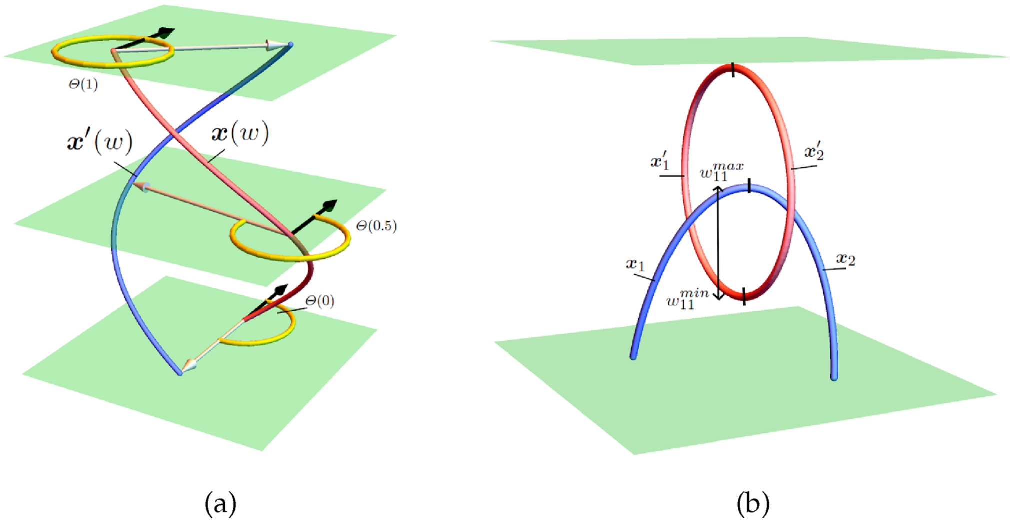

Figure 1. Illustrations of Euclidean winding quantities. (*a*) Winding of $\boldsymbol{x}'$ (blue) continuously measured by $\boldsymbol{x}$ (red) at each S_w (green) with respect to a fixed direction (black), resulting in the accumulated angular change (yellow) $\Theta = \int \omega_{\mathrm{E}}\, \mathrm{d}w$. (*b*) Example of curves that are not globally w-monotonic but whose winding can be unambiguously measured according to [11]; see also appendix A. Here, curves $\boldsymbol{x}$ (blue) and $\boldsymbol{x}'$ (red) are respectively split into w-monotonic subcurves $\boldsymbol{x}_1, \boldsymbol{x}_2, \boldsymbol{x}_1', \boldsymbol{x}_2'$, and $[w_{11}^{\min}, w_{11}^{\max}]$ is a mutually w-monotonic subinterval.

The *Euclidean winding rate* ω_{E} can be used to elucidate the topological significance of (1.7); e.g. [9,12,13]. In V_{E}, for a pair of w-parameterized, non-intersecting curves $\boldsymbol{x}(w) = (x, y, w)$ and $\boldsymbol{x}'(w) = (x', y', w)$, one can define ω_{E} by

$$\omega_{\mathrm{E}}(w; \boldsymbol{x}, \boldsymbol{x}') \equiv \frac{\mathrm{d}}{\mathrm{d}w} \arctan\left(\frac{y - y'}{x - x'}\right) = \frac{(x - x')(\dot{y} - \dot{y}') - (\dot{x} - \dot{x}')(y - y')}{(x - x')^2 + (y - y')^2}, \tag{1.8}$$

where $\dot{(\,)} \equiv \mathrm{d}/\mathrm{d}w$. As shown in figure 1*a*, ω_{E} can be understood as the angular velocity of $\boldsymbol{x}'$ measured on S_w by an observer co-moving with $\boldsymbol{x}$ (§2a for details). Writing $B_w \equiv \hat{\boldsymbol{e}}_w \cdot \boldsymbol{B}$, equation (1.7) can be written in terms of the Euclidean winding rate ω_{E} of $\boldsymbol{B}$-lines as

$$H^{\mathrm{W}}(\boldsymbol{B}) = \frac{1}{2\pi} \int_0^1 \int_{S_w} \int_{S_w} \omega_{\mathrm{E}}(w; \boldsymbol{x}, \boldsymbol{x}') B_w(\boldsymbol{x}) B_w(\boldsymbol{x}')\, \mathrm{d}^2\boldsymbol{x}'\, \mathrm{d}^2\boldsymbol{x}\, \mathrm{d}w\,. \tag{1.9}$$

Note that all $\boldsymbol{B}$-lines, whether globally w-monotonic or not, contribute to (1.9), since the signs of the normal magnetic field B_w consistently modify the Euclidean winding rate ω_{E} to retain the topological significance [9,11]. Figure 1*b* illustrates a toy example and interested readers are referred to appendix A for a review. Hence, it suffices for our present purpose to assume henceforth that all curves are w-monotonic.

Recently, the topological definition of helicity in terms of winding has been generalized to magnetically open Euclidean tubular domains (homoeomorphic to V_E) by Prior & Yeates [14], and to magnetically open spherical domains (foliated by concentric spheres) by Xiao *et al.* [15]. A crucial step in the latter case is to construct the intrinsic winding of spherical curves that accounts for both the domain topology (compactness) as well as the domain geometry (non-vanishing curvature). In particular, the Dirac belt-trick specific to spherical domains allows curves to be continuously disentangled with endpoints fixed and without crossing each other. Nevertheless, when integrated over the entire field, winding helicity remains invariant under ideal magnetohydrodynamic (MHD) deformation (continuous non-intersecting deformation, or *isotopy*, all $\boldsymbol{B}$-lines).

royalsocietypublishing.org/journal/rspa *Proc. R. Soc. A* **481:** 20240152

It is natural to investigate if such a winding-based definition of helicity can be further extended to magnetically open periodic domains of the form $V_\mathrm{p} \equiv \mathbb{T}^2 \times [0,1]$ where

$$\mathbb{T}^2 \equiv \mathbb{R}^2/\mathbb{Z}^2 = \{(x,y) : x \sim x+1, y \sim y+1\}, \tag{1.10}$$

is a doubly periodic square homoeomorphic to a 2-torus, and V_p is homoeomorphic to a foliation of concentric two-tori (with finite non-vanishing areas). To avoid unnecessary complications due to curvature, the choice V_p is intrinsically flat. Periodic domains correspond to the commonly used three-dimensional 'Cartesian boxes' with periodic boundary conditions in two lateral dimensions in analytical and numerical studies of (magneto)hydrodynamics (e.g. [16,17]). Also, such geometry is closely related to domains consisting of infinitely repeating units, applicable to biological sciences, polymer physics and crystallography (e.g. the introduction in [18]).

However, this has remained an open problem since Berger's attempt [19] in 1996 although progress has been reported in multiple directions. Panagiotou [18] studied the winding of curves in periodic domains using infinite sums of Euclidean winding, while not providing *ab initio* justification for the summation order, nor accounting for the compact nature of the domain. Pfefferlé *et al*. [20] and MacTaggart & Valli [21] independently proposed a generalization of relative helicity to multiply connected domains using de Rham cohomology, which includes periodic domains as a special case but yields no topological interpretation.

In this work, we present a solution to this open problem, i.e. a topological definition of helicity in open periodic domains V_p in terms of winding of $\boldsymbol{B}$-lines. First, in §2, we propose a definition of periodic winding of planar curves, which, in complex notation, reads as

$$\omega_\mathrm{p}(t;\gamma,\gamma') = \mathrm{Im}\left[\left(\zeta(z) - \pi\bar{z}\right)\frac{\mathrm{d}z}{\mathrm{d}t}\right], \tag{1.11}$$

where $\gamma,\gamma' : [0,1] \to \mathbb{T}^2$ are curves such that $\gamma(t) \neq \gamma'(t)$ for all $t \in [0,1]$ and $z \equiv \gamma - \gamma'$. Also, $\zeta(z)$ is the Weierstrass zeta function on $\mathbb{T}^2$ and the term $-\pi\bar{z}$ guarantees the double-periodicity of ω_p. Two examples are given in §3 to demonstrate properties of the periodic winding quantities.

Then, in §4, we analyse the topological implications of the periodic domains V_p by identifying, in proposition 1, the periodic winding gauge $\boldsymbol{A}^\mathrm{W}$ that satisfies not only (1.6) but also

$$\int_{V_\mathrm{p}} \boldsymbol{A}_0^\mathrm{W} \cdot \nabla \times \boldsymbol{A}_0^\mathrm{W}\, \mathrm{d}V = 0, \quad \text{where} \quad \boldsymbol{A}_0^\mathrm{W}(w) \equiv \int_{\mathcal{S}_w} \boldsymbol{A}^\mathrm{W}\, \mathrm{d}A \tag{1.12}$$

is the *harmonic fluxes* of $\boldsymbol{A}^\mathrm{W}$ on each $\mathcal{S}_w \equiv \mathbb{T}^2 \times \{w\}$. The extra condition (1.12) effectively removes helicity generated by $\boldsymbol{A}_0^\mathrm{W}$ and $\boldsymbol{B}_0$, which are present due to the domain topology.

In §5, one obtains the periodic winding helicity $H^\mathrm{W}(\boldsymbol{B})$ by using $\boldsymbol{A}^\mathrm{W}$ in (1.5) and replacing V_E with V_p. The main result, theorem 1, will then be proved to express $H^\mathrm{W}(\boldsymbol{B})$ as the total, flux-weighted, periodic winding of $\boldsymbol{B}$-lines, analogous to the Euclidean results:

$$H^\mathrm{W}(\boldsymbol{B}) = \frac{1}{2\pi}\int_0^1 \int_{\mathcal{S}_w}\int_{\mathcal{S}'_w} \omega_\mathrm{p}(w;\gamma,\gamma') B_w(z) B_w(z')\, \mathrm{d}A_{z'}\, \mathrm{d}A_z\, \mathrm{d}w, \tag{1.13}$$

where $\mathrm{d}A_z$ is the complex equivalent of $\mathrm{d}A = \mathrm{d}^2\boldsymbol{x}$ and similarly for $\mathrm{d}A_{z'}$. The extension to non-monotonic curves proceeds as described in appendix A.

In §6, key properties of periodic winding helicity (1.13) are proved, including its time-invariance under ideal MHD evolution, its relationship to existing Fourier approaches and the geometrical significance of gauge transformations. We end in §7 by discussing possible topological definitions of helicity in other domains that are beyond the scope of this article.

2. Winding in planar periodic domains

(a) Non-periodic winding

We first review the concept of the winding of curves in planar Euclidean, i.e. non-periodic, domains using a complex formulation by identifying $\mathbb{R}^2$ as $\mathbb{C}$. This is inspired by [22], which will benefit our subsequent periodic extension. Let $\gamma : [0,1] \to \mathbb{C} \setminus \{0\}$ be a smooth curve, and, unless otherwise stated, we assume it is either open or closed. Then, the *non-periodic winding angle* $\Theta_{\mathrm{E}}(t;\gamma)$ of $z=\gamma(t)$ about $z=0$ can be defined as

$$\Theta_{\mathrm{E}}(t;\gamma) \equiv \int_0^t \omega_{\mathrm{E}}(\tilde{t};\gamma)\,\mathrm{d}\tilde{t}\,, \quad \text{where} \quad t \in [0,1], \tag{2.1}$$

and the *non-periodic winding rate* $\omega_{\mathrm{E}}(t;\gamma)$ in (1.8) may be written as

$$\omega_{\mathrm{E}}(t;\gamma) \equiv \frac{\mathrm{d}}{\mathrm{d}t}\,\mathrm{Im}[\log z(t)] = \mathrm{Im}\left(\frac{1}{z}\frac{\mathrm{d}z}{\mathrm{d}t}\right). \tag{2.2}$$

Here, log is assumed to be defined continuously on the associated Riemann surface. Equivalently, using the principal argument Arg, we can write (2.1) as:

$$\Theta_{\mathrm{E}}(t;\gamma) = \mathrm{Arg}[z(t)] - \mathrm{Arg}[z(0)] + N(t), \tag{2.3}$$

where N is the signed number of full winding of γ about $z=0$.

For a pair of curves $\gamma, \gamma' : [0,1] \to \mathbb{C}$ such that $\gamma(t) \neq \gamma'(t)$ for all $t \in [0,1]$, we then define the *non-periodic pairwise winding rate* $\omega_{\mathrm{E}}(t;\gamma,\gamma')$ between γ and γ' as

$$\omega_{\mathrm{E}}(t;\gamma,\gamma') \equiv \frac{1}{2}[\omega_{\mathrm{E}}(t;\gamma-\gamma') + \omega_{\mathrm{E}}(t;\gamma'-\gamma)], \tag{2.4}$$

which is by definition symmetric in γ and γ'. Note that, from (2.2), it is clear that

$$\omega_{\mathrm{E}}(t;\gamma-\gamma') = \omega_{\mathrm{E}}(t;\gamma'-\gamma), \tag{2.5}$$

so that

$$\omega_{\mathrm{E}}(t;\gamma,\gamma') = \omega_{\mathrm{E}}(t;\gamma-\gamma') = \omega_{\mathrm{E}}(t;\gamma'-\gamma). \tag{2.6}$$

When written in Cartesian coordinates, (2.4) is identical to (1.8), albeit notationally more compact. Interested readers are referred to appendix A for a review of non-periodic winding for general spatial curves from [11] with relationship to the Gauss linking integral.

(b) Periodic winding

We identify the planar doubly periodic domain $\mathbb{T}^2$ as $\mathcal{S} \equiv \mathbb{C}/\mathbb{Z}[\mathrm{i}]$ in complex coordinates, where $\mathbb{Z}[\mathrm{i}] \equiv \{n = n_x + \mathrm{i}n_y : n_x, n_y \in \mathbb{Z}\}$ are the Gaussian integers. Translation invariance allows us to assume without loss of generality that $\mathcal{S}$ is centred at $z=0$. Let $\gamma : [0,1] \to \mathcal{S} \setminus \{0\}$ be a smooth curve, then for any $n \in \mathbb{Z}[\mathrm{i}]$, a *periodic image* γ_n of γ is defined as

$$\gamma_n \equiv \gamma + n : [0,1] \to \mathbb{C} \setminus \{0\}\,. \tag{2.7}$$

Examples of periodic images are shown in figure 2, which will be discussed further in §3.

It is intuitive to postulate that the *periodic winding rate*, denoted $\omega_{\mathrm{p}}(t;\gamma)$, of γ about $z=0$, could be defined as the sum of non-periodic winding $\omega_{\mathrm{E}}(t;\gamma_n)$ over all periodic images γ_n of γ, i.e.

$$\sum_{n\in\mathbb{Z}[\mathrm{i}]} \mathrm{Im}\left[\frac{1}{z+n}\frac{\mathrm{d}}{\mathrm{d}t}(z+n)\right] = \mathrm{Im}\left[\left(\sum_{n\in\mathbb{Z}[\mathrm{i}]}\frac{1}{z+n}\right)\frac{\mathrm{d}z}{\mathrm{d}t}\right]. \tag{2.8}$$

However, it is well known that the infinite sum on the right side of (2.8) is ill-defined and can yield arbitrary values by changing the summation order, since it converges only conditionally

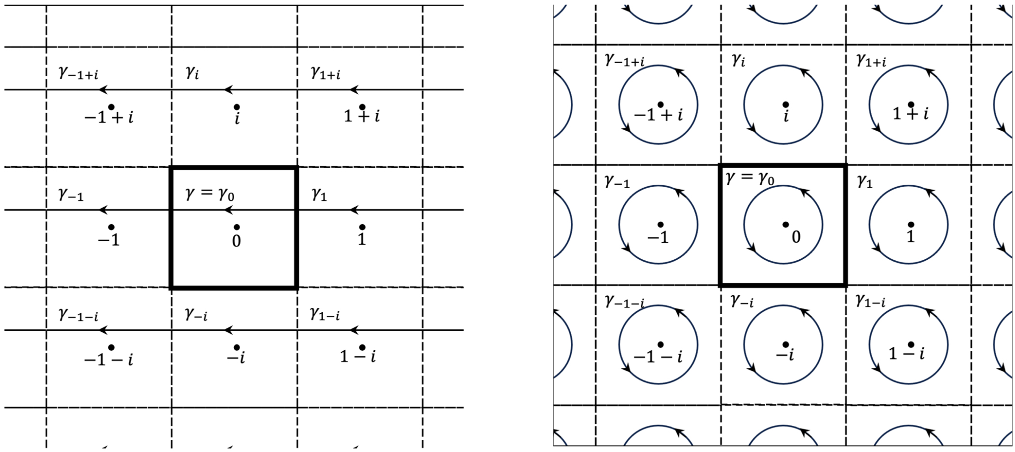

(a). Line-point winding
$\gamma\colon z=-t+0.5+0.25i$

(b). Circle-point winding
$\gamma\colon z=0.25e^{2\pi it}$

Figure 2. Periodic images γ_n of the curve γ for examples of (*a*) line-point and (*b*) circle-point winding in the planar periodic domain $\mathcal{S}$ (marked by the bold outline).

[23]. To retain the singular behaviour of (2.8) that generates winding while ensuring finiteness and single-valuedness, we apply the Mittag–Leffler theorem [23] so that

$$\sum_{n\in\mathbb{Z}[\mathrm{i}]}\frac{1}{z+n}\xrightarrow{\text{M.-L.}}\zeta(z)\equiv\frac{1}{z}+\sum_{\substack{n\in\mathbb{Z}[\mathrm{i}]\\ n\neq 0}}\left(\frac{1}{z-n}+\frac{1}{n}+\frac{z}{n^2}\right),\tag{2.9}$$

where $\zeta(z)$ is the *Weierstrass zeta function* [24] defined on $\mathcal{S}$. The additional terms now guarantee absolute and uniform convergence. Geometrically, O'Neil [25] showed that $\zeta(z)$ is equivalent to the limit of a finite sum over $C_R\equiv\{|z|\leq R\}$ with $R\to\infty$:

$$\zeta(z)=\lim_{R\to\infty}\sum_{\substack{n\in\mathbb{Z}[\mathrm{i}]\\ |n|<R}}\frac{1}{z+n}.\tag{2.10}$$

Here, the radially symmetric order of summation is *necessary* for the above equality to hold, as assumed in, e.g. Panagiotou [18], to demonstrate convergence explicitly. Our use of the Mittag–Leffler theorem provides a closed-form expression that is automatically convergent.

A further modification, however, is needed due to the compactness of $\mathcal{S}$, since (2.9) still fails to be doubly periodic due to Legendre's relations [24] on $\mathcal{S}$:

$$\zeta(z+1)=\zeta(z)+\pi,\qquad \zeta(z+\,)=\zeta(z)-\pi.\tag{2.11}$$

To restore periodicity, we need to remove a linear gradient $\pi\bar{z}$ from $\zeta(z)$ so that,

$$\zeta(z)\longrightarrow\zeta(z)-\pi\bar{z},\tag{2.12}$$

which is also the unique, non-trivial term that can be added to achieve this due to Liouville's theorem. In crystallography literature, e.g. [26], the extra term $-\pi\bar{z}$ is referred to as the existence of a uniform background of counter source, or 'jellium', to neutralize that of $z=0$. Alternatively, it is interpreted as the compensation for the far-field contribution of the finite sum (2.10) in [27].

Thus, the definition of *periodic winding rate* $\omega_{\mathrm{p}}(t;\gamma)$ is modified from the intuitive sum (2.8) to

$$\omega_{\mathrm{p}}(t;\gamma) \equiv \mathrm{Im}\left[(\zeta(z) - \pi\bar{z})\frac{\mathrm{d}z}{\mathrm{d}t}\right]. \tag{2.13}$$

Using (2.10), it can be written in terms of the non-periodic winding rates ω_{E}, (2.2), as follows:

$$\omega_{\mathrm{p}}(t;\gamma) = \lim_{R\to\infty} \sum_{\substack{n\in\mathbb{Z}[\mathrm{i}] \\ |n|<R}} \left[\left(1 - \frac{\pi|z+n|^2}{N_R}\right)\omega_{\mathrm{E}}(t;\gamma_n)\right], \tag{2.14}$$

where $N_R = \pi R^2 + O(R^{14/22})$ is the number of lattice points within C_R; see [28] for details.

For curves $\gamma, \gamma' : [0,1] \to \mathcal{S}$ such that $\gamma(t) \neq \gamma'(t)$ for all $t \in [0,1]$, the *pairwise periodic winding rate* $\omega_{\mathrm{p}}(t;\gamma,\gamma')$ can be similarly defined as

$$\omega_{\mathrm{p}}(t;\gamma,\gamma') \equiv \frac{1}{2}[\omega_{\mathrm{p}}(t;\gamma-\gamma') + \omega_{\mathrm{p}}(t;\gamma'-\gamma)], \tag{2.15}$$

which is manifestly symmetric in γ and γ'. Also, translation invariance ensures that (2.15) is well-defined. From (2.2), we have

$$\omega_{\mathrm{p}}(t;\gamma-\gamma') = \omega_{\mathrm{p}}(t;\gamma'-\gamma), \tag{2.16}$$

so that

$$\omega_{\mathrm{p}}(t;\gamma,\gamma') = \omega_{\mathrm{p}}(t;\gamma-\gamma') = \omega_{\mathrm{p}}(t;\gamma'-\gamma). \tag{2.17}$$

We thus propose that the periodic winding rates, (2.13) and (2.15), provide natural generalizations to the non-periodic quantities (2.2) and (2.4).

(c) Winding and Green's functions for Laplacians

Here, we demonstrate how the non-periodic winding rate ω_{E} and its periodic generalization ω_{p} can be unified into a single expression using Green's functions for Laplacian of the respective domain. This observation will be crucial in relating winding to helicity in §4.

Recall that the Euclidean *Green's function* $G_{\mathrm{E}}(z,z')$ for Laplacian is defined as the solution to the following Poisson's equation on $S = \mathbb{C}$:

$$\Delta_z G_{\mathrm{E}}(z,z') = \delta(z-z'), \tag{2.18}$$

or the periodic Green's function $G_{\mathrm{p}}(z,z')$ if it is defined on $\mathcal{S} = \mathbb{C}/\mathbb{Z}[\mathrm{i}]$:

$$\Delta_z G_{\mathrm{p}}(z,z') = \delta(z-z') - 1/\mathrm{Area}(\mathcal{S}). \tag{2.19}$$

Here, $\delta(z-z')$ is the Dirac function with the singularity located at $z = z'$, and $\Delta_z = 4\partial_z\partial_{\bar{z}} = 4\partial_{\bar{z}}\partial_z$ is the Laplacian with respect to z using Wirtinger complex derivatives

$$\partial_z \equiv (\partial_x - \partial_y)/2, \quad \partial_{\bar{z}} \equiv (\partial_x + \partial_y)/2. \tag{2.20}$$

Since $\mathcal{S}$ is compact and boundaryless, it is more precise to refer to $G_{\mathrm{p}}(z,z')$ as the *generalized* [29], or *source-neutral* [26], *Green's function*. Also, the inclusion of the term $1/\mathrm{Area}(\mathcal{S}) = 1$ guarantees that compatibility due to Stokes' theorem is satisfied by G_{p}, i.e.

$$\int_{\mathcal{S}} G_{\mathrm{p}}(z,z')\,\mathrm{d}A_z = 0, \tag{2.21}$$

where $\mathrm{d}A_z = \mathrm{d}\bar{z} \wedge \mathrm{d}z\,/(2)$ is the area form on $\mathbb{C}$ as the complex equivalent of $\mathrm{d}A = \mathrm{d}x \wedge \mathrm{d}y$.

Explicit expressions of $G_{\mathrm{E}}(z,z')$ and $G_{\mathrm{p}}(z,z')$ are given by, e.g. Lin & Wang [30]:

$$G_{\mathrm{E}}(z,z') = \frac{1}{2\pi}\log|z-z'|, \tag{2.22}$$

$$G_{\mathrm{p}}(z,z') = \frac{1}{2\pi}\log|\vartheta_1(z-z')| - \frac{1}{2}\left[\mathrm{Im}(z-z')\right]^2, \tag{2.23}$$

where $\vartheta_1(z)$ is the *first Jacobi theta function* on $\mathcal{S}$ defined by, e.g. according to Whittaker & Watson [24],

$$\vartheta_1(z) = 2\sum_{n=0}^{\infty}(-1)^n \mathrm{e}^{-\pi(n+\frac{1}{2})^2}\sin\left[(2n+1)\pi z\right]. \tag{2.24}$$

Both (2.22) and (2.23) are translation invariant and symmetric in z and z', allowing one to set $(z-z')\to z$, so Green's functions can be regarded as univariate without ambiguity. Also, the derivatives of the Green's functions are given by [24]

$$4\pi\partial_z G_{\mathrm{E}}(z) = 1/z, \tag{2.25}$$

$$4\pi\partial_z G_{\mathrm{p}}(z) = \zeta(z) - \pi\bar{z}. \tag{2.26}$$

For reference, both derivatives are visualized in figure 3.

Comparing (2.25) with (2.2) and (2.26) with (2.13), the periodic (with subscript $\mathrm{k}=\mathrm{p}$) and non-periodic (with subscript $\mathrm{k}=\mathrm{E}$) winding rates can be unified into a single expression

$$\omega_{\mathrm{k}}(t;\gamma) = 4\pi\,\mathrm{Im}\left[\partial_z G_{\mathrm{k}}(z)\frac{\mathrm{d}z}{\mathrm{d}t}\right]. \tag{2.27}$$

We can also define its integral as the *winding number*, denoted $L_{\mathrm{k}}(t;\gamma)$, as

$$L_{\mathrm{k}}(\gamma) \equiv \frac{1}{2\pi}\int_0^1 \omega_{\mathrm{k}}(t;\gamma)\,\mathrm{d}t, \tag{2.28}$$

where the factor of $1/(2\pi)$ is customary. It follows from (2.27) that

$$L_{\mathrm{k}}(\gamma) = 2\,\mathrm{Im}\int_\gamma \partial_z G_{\mathrm{k}}(z)\,\mathrm{d}z. \tag{2.29}$$

3. Examples of periodic winding of planar curves

In this section, we compute periodic (with subscript p) and non-periodic (with subscript E) winding quantities for the examples shown in figure 2, i.e. winding of either a line in §3a or a circle in §3b about $z=0$ (formally a degenerate line as $\{z=0\}\times[0,1]$). Numerical and analytical computations are confirmed to coincide for winding numbers using (2.28) and (2.29), respectively.

(a) Line-point winding

Certain lines cannot be continuously contracted to a point in periodic domains, which manifests the non-trivial domain topology and will later be associated with the non-vanishing harmonic fluxes in §4. For simplicity, we consider horizontal lines γ of the form

$$\gamma: z = -t + 0.5 + \mathrm{i}a, \quad \text{where } t\in[0,1],\ a\in[-0.5,0.5]\setminus\{0\}, \tag{3.1}$$

and compute their periodic and non-periodic winding about $z=0$. The case $a=0.25$ is shown in figure 2*a*, and relevant winding quantities are plotted in figure 4.

In this example, since $\mathrm{d}z/\mathrm{d}t=-1$, winding rates ω_{p} and ω_{E} are, up to a sign, the respective imaginary parts of (2.25) and (2.26). As shown in figure 4*a*, we observe that $|\omega_{\mathrm{p}}|<|\omega_{\mathrm{E}}|$.

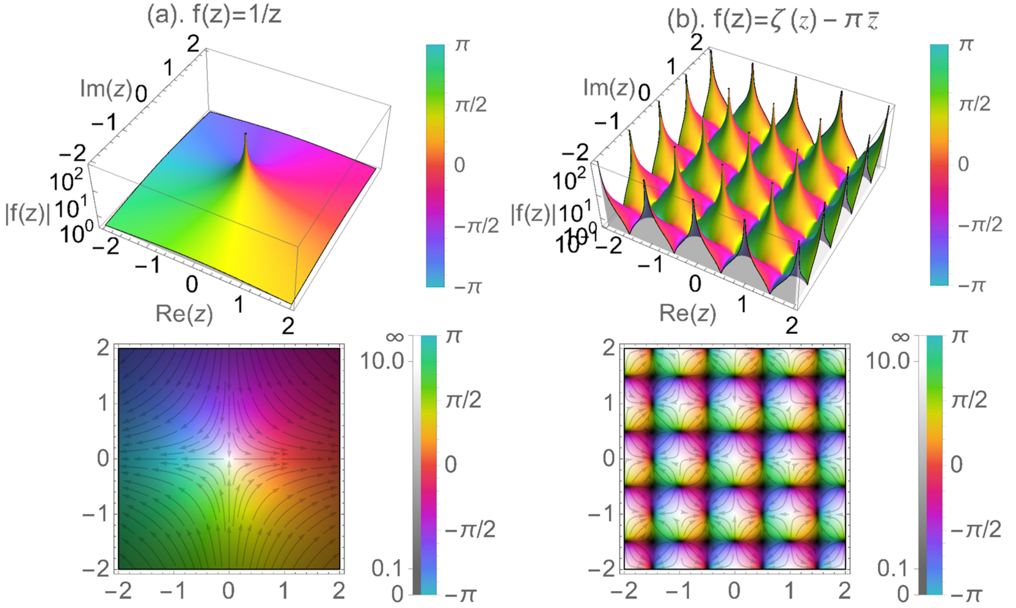

Figure 3. (*a*, *b*) Three-dimensional (top row) and two-dimensional/streamline (bottom row) plots of derivatives of Green's functions (2.25) and (2.26) that are used in defining winding rates (2.27). Colours and grey shades, respectively, indicate the complex phase and modulus.

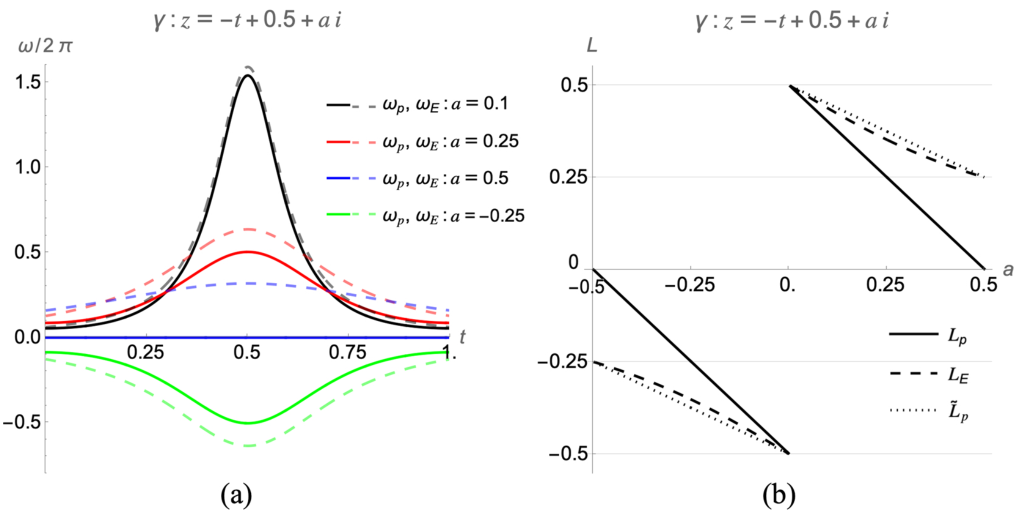

Figure 4. (*a*) Winding rates ω_p, ω_E against curve parameter t, and (*b*) winding numbers L_p, L_E of lines (3.1) about $z=0$ against vertical positions a. Periodic (or non-periodic) quantities are plotted in solid (or dashed), same for figure 6. The quantity $\tilde{L}_\mathrm{p}$, (3.4), is also shown in comparison.

In particular, at $a=\pm 0.5$, we have $\omega_\mathrm{p}=0$ and no overall periodic winding is measured, when the line simultaneously traverses the lower and upper domain boundaries with the same rate but in opposite directions. This could be interpreted as some 'localizing' effect from periodicity.

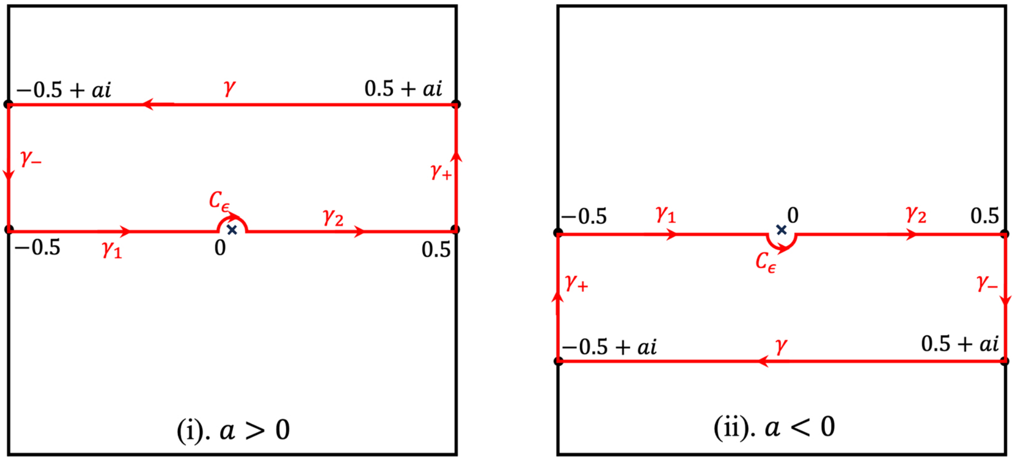

Figure 5. Contours used to evaluate $\int_\gamma \zeta(z)\,\mathrm{d}z$ in (3.3). Note that $\mathrm{Res}_{z=0}\zeta(z) = 1$, $\int_{\gamma_1} \zeta(z)\,\mathrm{d}z = -\int_{\gamma_2} \zeta(z)\,\mathrm{d}z$ from parity and $\int_{\gamma_+} \zeta(z)\,\mathrm{d}z + \int_{\gamma_-} \zeta(z)\,\mathrm{d}z = -\mathrm{i}a\pi$ from quasi-periodicity (2.11).

Figure 4*b* plots numerically computed winding numbers, L_p and L_E, using (2.28) for possible values of a, which is verified analytically as follows. For L_E, it is easy to show from (2.29) that

$$L_\mathrm{E}(a) = \frac{1}{2\pi}\mathrm{Arg}\left(\frac{2\mathrm{i}a-1}{2\mathrm{i}a+1}\right). \tag{3.2}$$

For L_p, the contour integral in figure 5 gives $\int_\gamma \zeta(z)\,\mathrm{d}z = -\mathrm{i}a\pi + \pi$ and direct integration yields $\int_\gamma \bar{z}\,\mathrm{d}z = -\mathrm{i}a$. It then follows from (2.29) that

$$L_\mathrm{p}(a) = \frac{1}{2}\mathrm{sgn}(a) - a. \tag{3.3}$$

In addition, to demonstrate the necessity of including the compactness correction term (2.29), we considered the quantity $\tilde{L}_\mathrm{p}$ defined by

$$\tilde{L}_\mathrm{p}(a) \equiv L_\mathrm{p}(a) - \frac{1}{2\pi}\int_\gamma -\pi\bar{z}\ \mathrm{d}z = \frac{1}{2}\mathrm{sgn}(a) - \frac{a}{2}. \tag{3.4}$$

Note that, across the identified boundaries $a = \pm 0.5$, only the periodic winding number L_p has the desired continuity. Also, as the line passes through the origin, a jump in the winding number at $a = 0$ and the generation of 'net winding' is observed in all cases, albeit also achievable via an isotopy by moving the line across $a = \pm 0.5$. This suggests the inherent impossibility of defining an isotopy-invariant measure of winding in periodic domains, which was also reported for the Dirac belt-trick deformation in [15] when defining similar winding measures in spherical domains.

(b) Circle-point winding

Next, we consider circles—the simplest closed planar curves—of the form,

$$\gamma : z = r\mathrm{e}^{2\pi\mathrm{i}t}, \quad \text{where } t \in [0,1],\ r \in (0, 0.5] \cup \{1/\sqrt{2}\}, \tag{3.5}$$

and compute their periodic and non-periodic winding about $z = 0$. The case $r = 0.25$ is shown in figure 2*b*, and relevant winding quantities are plotted in figure 6. For the non-periodic case, it is clear that, regardless of the value of r, we have

$$\omega_\mathrm{E} = 2\pi, \qquad L_\mathrm{E} = 1, \tag{3.6}$$

since γ encircles $z = 0$ exactly once at this constant rate.

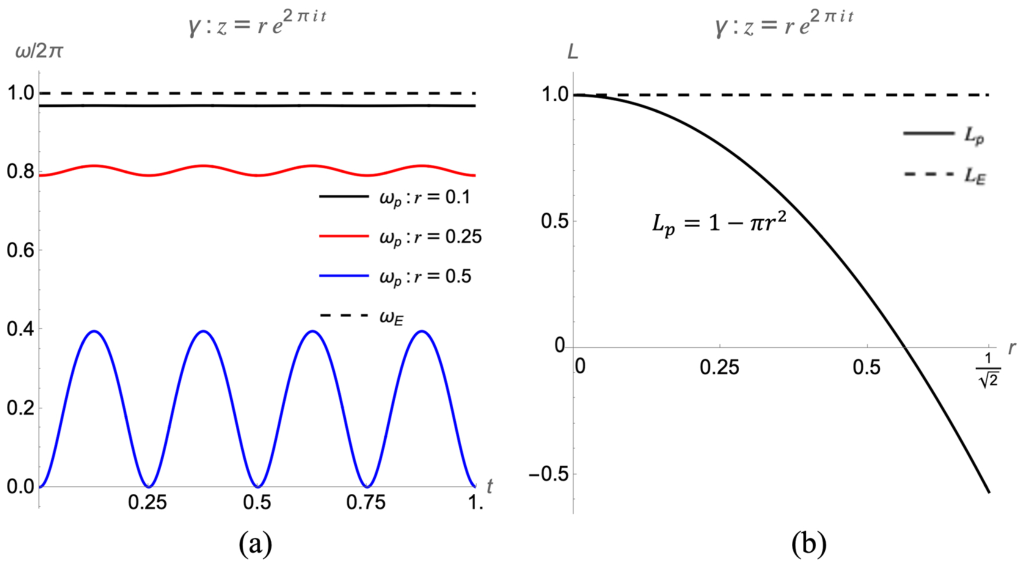

Figure 6. (*a*) Winding rates $\omega_\mathrm{p}, \omega_\mathrm{E}$ against curve parameter t, and (*b*) winding numbers $L_\mathrm{p}, L_\mathrm{E}$ of circles (3.5) about $z = 0$ against radius r. Note that, $r \in (1/2, 1/\sqrt{2})$ is ill-defined and ignored.

By contrast, as shown in figure 6*a*, the periodic winding rate experiences a similar 'localizing' effect, or $\omega_\mathrm{p} < \omega_\mathrm{E}$. When $r = 0.5$, γ passes through with the zeros of $\partial_z G_\mathrm{p}$ (cf. figure 3*b*) and $\omega_\mathrm{p} = 0$. This corresponds to the cancellation of equal and opposite winding simultaneously generated by the periodic images of γ. The analytical expression of the periodic winding number L_p can be obtained by, noting that $\int_\gamma \bar{z}\,\mathrm{d}z = 2\pi r^2$,

$$L_\mathrm{p}(r) = \frac{1}{2\pi}\,\mathrm{Im}\oint_\gamma (\zeta(z) - \pi\bar{z})\,\mathrm{d}z = 1 - \pi r^2. \tag{3.7}$$

While L_p is undefined for $r \in (1/2, \sqrt{2}/2)$ due to the ill-defined transversal direction, it can still be computed at the isolated point $r = \sqrt{2}/2$. As illustrated in figure 7, this case realizes the 'inside-out' transition, or a reversal of the winding direction [19], and hence also violates the usual isotopy-invariance satisfied by non-periodic winding. Also, the use of contour integration in both examples suggests that the winding numbers of any slightly distorted circle or line (with endpoints unchanged) will remain identical, although the relevant winding rates will be different.

Despite the aforementioned peculiarities for individual pairs of curves, we will show next that the flux-weighted periodic winding over all such pairs, i.e. winding helicity, is in fact invariant under ideal MHD deformations.

4. Magnetic fields in periodic domains

In this section, we review the non-trivial topology of periodic domains and study its implications on vector fields defined therein. Specifically, we identify a vector potential, the winding gauge and derive a generalized version of the poloidal–toroidal decomposition of magnetic fields, in preparation for proving the main theorem in §5 that relates helicity to winding.

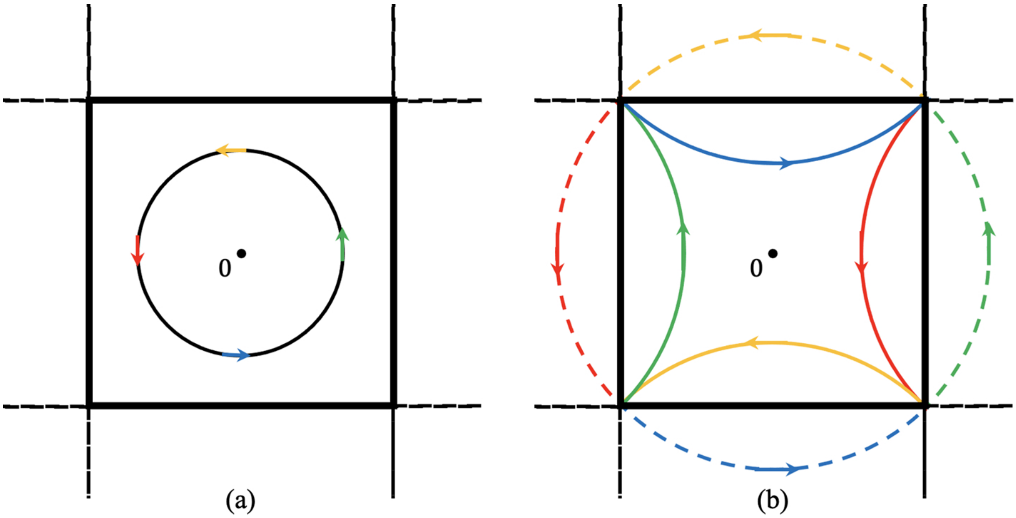

Figure 7. A reversal of the direction of winding: (*a*) counterclockwise when $r < 1/2$ and (*b*) clockwise when $r = 1/\sqrt{2}$.

(a) Topology of periodic domains

Recall that the three-dimensional (doubly) periodic domain is defined as $V_\mathrm{p} = \mathcal{S} \times [0, 1]$ with $\mathcal{S} = \mathbb{T}^2$ and its non-periodic counterpart as $V_\mathrm{E} = S \times [0, 1]$ with $\mathcal{S} = \mathbb{R}^2$, the additional dimension referred to as the *vertical* direction. Via homotopy, V_p is topologically equivalent to $\mathcal{S}$.

Let $\Omega(V_\mathrm{p})$ be the space of smooth, square-integrable vector fields defined on V_p, then, using the usual differential operators div, grad, curl, the following subspaces of $\Omega(V_\mathrm{p})$

$$H^1(V_\mathrm{p}) \equiv \ker[\mathrm{curl}(V_\mathrm{p})] \,/\, \mathrm{im}[\mathrm{grad}(V_\mathrm{p})], \tag{4.1}$$

$$H^2(V_\mathrm{p}) \equiv \ker[\mathrm{div}(V_\mathrm{p})] \,/\, \mathrm{im}[\mathrm{curl}(V_\mathrm{p})], \tag{4.2}$$

are defined, respectively, as the *first* and *second de Rham cohomology groups*, e.g. [31,32]. The topology of V_p is precisely characterized by (4.1) and (4.2) and it is well known that

$$H^1(V_\mathrm{p}) = \mathrm{span}\{\hat{\boldsymbol{e}}_x, \hat{\boldsymbol{e}}_y\}, \quad H^2(V_\mathrm{p}) = \mathrm{span}\{\hat{\boldsymbol{e}}_w\}, \tag{4.3}$$

where $\{\hat{\boldsymbol{e}}_x, \hat{\boldsymbol{e}}_y, \hat{\boldsymbol{e}}_w\}$ are the usual Cartesian basis vectors in $\mathbb{R}^3$. By comparison, the non-periodic domain V_E has trivial topology (equivalent to $\mathbb{R}^2$), namely,

$$H^1(V_\mathrm{E}) = H^2(V_\mathrm{E}) = \{0\}. \tag{4.4}$$

For any $\boldsymbol{v} \in \Omega(V_\mathrm{p})$, its *harmonic flux*, or *zero-mode*, $\boldsymbol{v}_0 \in H^1(V_\mathrm{p})$, is defined by

$$\boldsymbol{v}_0(w) \equiv \langle \hat{\boldsymbol{e}}_x, \boldsymbol{v}\rangle\, \hat{\boldsymbol{e}}_x + \langle \hat{\boldsymbol{e}}_y, \boldsymbol{v}\rangle\, \hat{\boldsymbol{e}}_y, \tag{4.5}$$

where $\langle \cdot, \cdot \rangle$ is the surface average on $\mathcal{S}$, i.e. for any $\boldsymbol{a}, \boldsymbol{b} \in \Omega(V_\mathrm{p})$, we define

$$\langle \boldsymbol{a}, \boldsymbol{b} \rangle \equiv \int_{\mathcal{S}} \boldsymbol{a} \cdot \boldsymbol{b}\, \mathrm{d}A. \tag{4.6}$$

(b) Winding gauge for magnetic fields in periodic domains

In the periodic domain, V_{p}, let $\boldsymbol{B} \in \ker[\operatorname{div}(V_{\mathrm{p}})]$ be a *magnetic field*. Then, the non-trivial second cohomology group $H^2(V_{\mathrm{p}})$ implies that there exists some *vector potential* $\boldsymbol{A} \in \Omega(V_{\mathrm{p}})$ such that

$$\boldsymbol{B} = \nabla \times \boldsymbol{A} + \Phi\, \hat{\boldsymbol{e}}_w, \tag{4.7}$$

where Φ is the surface-averaged normal magnetic flux

$$\Phi \equiv \langle \hat{\boldsymbol{e}}_w, \boldsymbol{B} \rangle\,. \tag{4.8}$$

Note that, a magnetic field $\boldsymbol{B} \in \ker[\operatorname{div}(V_{\mathrm{E}})]$ in the non-periodic domain V_{E} can always be written

$$\boldsymbol{B} = \nabla \times \boldsymbol{A}, \tag{4.9}$$

for some $\boldsymbol{A} \in \Omega(V_{\mathrm{E}})$ due to the triviality of $H^2(V_{\mathrm{E}})$, even if it has $\Phi \neq 0$.

Since $\mathcal{S}$ is closed, to avoid violating Gauss's law for magnetism [20], we impose

$$\Phi = 0, \tag{4.10}$$

for magnetic fields in periodic domains, so that (4.9) also holds true. This allows us to identify a special choice, the *winding gauge* $\boldsymbol{A}^{\mathrm{W}}$, among all permissible vector potentials:

Proposition 1. *In the periodic domain* $V_{\mathrm{p}} = \mathcal{S} \times [0, 1]$, *for any given magnetic field* $\boldsymbol{B} \in \ker[\operatorname{div}(V_{\mathrm{p}})]$ *with* $\Phi = 0$, *there exists a vector potential* $\boldsymbol{A}^{\mathrm{W}}$ *of the form*

$$\boldsymbol{A}^{\mathrm{W}} = T\hat{\boldsymbol{e}}_w + \nabla \times (P\hat{\boldsymbol{e}}_w) + \boldsymbol{A}_0^{\mathrm{W}}, \tag{4.11}$$

such that, on each horizontal surface $\mathcal{S}_w \equiv \mathcal{S} \times \{w\}$, *the* poloidal *and* toroidal flux functions P *and* T, *satisfy*

$$\Delta_S P = -\hat{\boldsymbol{e}}_w \cdot \boldsymbol{B}, \tag{4.12}$$

$$\Delta_S T = -\hat{\boldsymbol{e}}_w \cdot \nabla \times \boldsymbol{B}; \tag{4.13}$$

and the harmonic flux $\boldsymbol{A}_0^{\mathrm{W}}(w) \equiv \fint_{\mathcal{S}_w} \boldsymbol{A}^{\mathrm{W}}\ \mathrm{d}A$, *defined in (4.5), satisfies*

$$\int_{V_{\mathrm{p}}} \boldsymbol{A}_0^{\mathrm{W}} \cdot \nabla \times \boldsymbol{A}_0^{\mathrm{W}}\ \mathrm{d}V = 0. \tag{4.14}$$

Proof. Applying the Hodge Decomposition Theorem for surfaces [33] to any admissible vector potential $\boldsymbol{A} \in \Omega(V_{\mathrm{p}})$ for $\boldsymbol{B}$ gives, on each $\mathcal{S}_w$, that

$$\boldsymbol{A} = A_w \hat{\boldsymbol{e}}_w - \hat{\boldsymbol{e}}_w \times \nabla_S P + \nabla_S g + \boldsymbol{A}^*. \tag{4.15}$$

The summands are mutually orthogonal with respect to $\langle \cdot, \cdot \rangle$ and are uniquely defined by:

$$A_w = \hat{\boldsymbol{e}}_w \cdot \boldsymbol{A}, \tag{4.16}$$

$$\Delta_S P = -\hat{\boldsymbol{e}}_w \cdot \nabla \times \boldsymbol{A}, \tag{4.17}$$

$$\Delta_S g = \nabla_S \cdot (\boldsymbol{A} - A_w \hat{\boldsymbol{e}}_w), \tag{4.18}$$

$$\boldsymbol{A}^* = \boldsymbol{A} - A_w \hat{\boldsymbol{e}}_w + \hat{\boldsymbol{e}}_w \times \nabla_S P - \nabla_S g. \tag{4.19}$$

Here, $\nabla_S = (\partial_x, \partial_y, 0)$ is the surface gradient and $\Delta_S = \nabla_S \cdot \nabla_S = \partial_x^2 + \partial_y^2$ is the surface Laplacian. By definition, we have $\hat{\boldsymbol{e}}_w \cdot \boldsymbol{A}^* = \nabla_S \cdot \boldsymbol{A}^* = \hat{\boldsymbol{e}}_w \cdot \nabla \times \boldsymbol{A}^* = 0$, which implies that

$$\boldsymbol{A}^* = A_x^*(w)\, \hat{\boldsymbol{e}}_x + A_y^*(w)\, \hat{\boldsymbol{e}}_y. \tag{4.20}$$

Consider a gauge transformation to $\boldsymbol{A}$ such that $\boldsymbol{A}' = \boldsymbol{A} + \boldsymbol{G}$ for some $\boldsymbol{G} \in \ker[\operatorname{curl}(V_{\mathrm{p}})]$. From (4.3), we know that $\boldsymbol{G}$ must take the form

$$\boldsymbol{G} = \nabla \chi + \boldsymbol{G}_0, \tag{4.21}$$

for some scalar function χ and constant vector $\boldsymbol{G}_0$ such that $\hat{\boldsymbol{e}}_w \cdot \boldsymbol{G} = 0$. Choosing $\chi = -g + f$ with an arbitrary function $f = f(w)$ gives

$$\boldsymbol{A}' = (A_w + \partial\chi/\partial w)\hat{\boldsymbol{e}}_w + \nabla \times (P\hat{\boldsymbol{e}}_w) + \boldsymbol{A}^* + \boldsymbol{G}_0, \tag{4.22}$$

where we used $-\hat{\boldsymbol{e}}_w \times \nabla_S P = \nabla \times (P\hat{\boldsymbol{e}}_w)$ since $\mathcal{S}_w$ has vanishing curvature.

Note that, P is manifestly invariant under gauge transformations and explicit computation verifies (4.12). Also, Stokes' theorem implies that $\int_{\mathcal{S}_w} \nabla \times (P\hat{\boldsymbol{e}}_w)\, \mathrm{d}A = \boldsymbol{0}$ on each $\mathcal{S}_w$. The condition (4.13) satisfied by T follows if we define

$$T \equiv A_w + \partial\chi/\partial w, \tag{4.23}$$

and use remaining degree of freedom in $f(w)$ to enforce, if necessary, $\int_{\mathcal{S}_w} \hat{\boldsymbol{e}}_w \cdot \boldsymbol{A}'\, \mathrm{d}A = \boldsymbol{0}$ on each $\mathcal{S}_w$. For (4.14), we can choose $\boldsymbol{G}_0$ according to

$$\boldsymbol{A}_0^{\mathrm{W}} \equiv \boldsymbol{A}^* + \boldsymbol{G}_0, \tag{4.24}$$

so that $\boldsymbol{A}_0^{\mathrm{W}}(w) = \int_{\mathcal{S}_w} \boldsymbol{A}^{\mathrm{W}}\, \mathrm{d}A$ is indeed the harmonic flux by identifying $\boldsymbol{A}^{\mathrm{W}} \equiv \boldsymbol{A}'$. ■

An immediate consequence of proposition 1 is a generalized version of poloidal–toroidal decomposition for magnetic fields in periodic domains:

Corollary 1. *In the winding gauge $\boldsymbol{A}^{\mathrm{W}}$, every magnetic field $\boldsymbol{B}$ in V_{p} can be written as*

$$\boldsymbol{B} = \nabla \times (T\hat{\boldsymbol{e}}_w) + \nabla \times \nabla \times (P\hat{\boldsymbol{e}}_w) + \boldsymbol{B}_0, \tag{4.25}$$

where the harmonic flux, $\boldsymbol{B}_0 \equiv \int_{\mathcal{S}_w} \boldsymbol{B}\, \mathrm{d}^2\boldsymbol{x}$, satisfies

$$\boldsymbol{B}_0 = \nabla \times \boldsymbol{A}_0^{\mathrm{W}}. \tag{4.26}$$

In our earlier work [15], see also Berger & Hornig [34], a similar derivation was presented in Cartesian and spherical domains that are both simply connected (with trivial H^1). Proposition 1 and corollary 1 hold in both cases but with

$$\boldsymbol{A}_0^{\mathrm{W}} = \boldsymbol{B}_0 = \boldsymbol{0}. \tag{4.27}$$

From (4.11), the winding gauge $\boldsymbol{A}^{\mathrm{W}}$ has vanishing surface divergence on each $\mathcal{S}_w$, namely,

$$\nabla_S \cdot \boldsymbol{A}^{\mathrm{W}} = 0. \tag{4.28}$$

Meanwhile, the global condition (4.14) ensures that

$$\int_{V_{\mathrm{p}}} \boldsymbol{A}_0^{\mathrm{W}} \cdot \boldsymbol{B}\, \mathrm{d}V = \int_{V_{\mathrm{p}}} \boldsymbol{A}_0^{\mathrm{W}} \cdot \boldsymbol{B}_0\, \mathrm{d}V + \int_0^1 \boldsymbol{A}_0^{\mathrm{W}} \cdot \left[\int_{\mathcal{S}_w} (\boldsymbol{B} - \boldsymbol{B}_0)\, \mathrm{d}^2\boldsymbol{x}\right] \mathrm{d}w = 0, \tag{4.29}$$

where the second term vanishes by definition of $\boldsymbol{B}_0$. This implies that, according to the original definition of helicity, (1.1), the harmonic flux $\boldsymbol{A}_0^{\mathrm{W}}$ has no helicity contribution in V_{p}. Further discussions on these properties can be found in §6b,c.

5. Winding helicity in periodic domains

(a) Statement and proof

Given a magnetic field $\boldsymbol{B}$ in the periodic domain $V_{\mathrm{p}} = \mathcal{S} \times [0, 1]$, we define the *periodic winding helicity* $H^{\mathrm{W}}(\boldsymbol{B})$ by substituting $\boldsymbol{A}^{\mathrm{W}}$ from proposition 1 in (1.1), i.e.

$$H^{\mathrm{W}}(\boldsymbol{B}) \equiv \int_{V_{\mathrm{p}}} \boldsymbol{A}^{\mathrm{W}} \cdot \boldsymbol{B}\, \mathrm{d}V. \tag{5.1}$$

We will, in theorem 1, establish a direct link between periodic winding helicity $H^{\mathrm{W}}(\boldsymbol{B})$ and the periodic winding of $\boldsymbol{B}$-lines (parameterized by $w \in [0, 1]$). Recall that the latter are defined by

$$\frac{\mathrm{d}\boldsymbol{x}}{\mathrm{d}w} = \frac{\boldsymbol{B}[\boldsymbol{x}(w)]}{B_w[\boldsymbol{x}(w)]}. \tag{5.2}$$

Theorem 1. *Periodic winding helicity $H^{\mathrm{W}}(\boldsymbol{B})$ in $V_{\mathrm{p}}=\mathbb{T}^2\times[0,1]$ is equivalent to the total, flux-weighted pairwise periodic winding of* **B**-*lines, i.e.*

$$H^{\mathrm{W}}(\boldsymbol{B})=\frac{1}{2\pi}\int_0^1\int_{\mathcal{S}_w}\int_{\mathcal{S}'_w}\omega_{\mathrm{p}}(\gamma,\gamma')B_w(z)B_w(z')\,\mathrm{d}A_{z'}\,\mathrm{d}A_z\,\mathrm{d}w, \tag{5.3}$$

where $w\in[0,1]$ labels each horizontal slice $\mathcal{S}_w\equiv\mathbb{T}^2\times\{w\}$ with coordinates $z(w)=x(w)+\mathrm{i}y(w)$, and γ,γ' are the respective **B**-*lines through z,z'. The periodic winding rate ω_{p} is given in* (2.13).

Proof. It follows from (4.29) that it suffices to compute

$$H^{\mathrm{W}}(\boldsymbol{B})=\int_{V_{\mathrm{p}}}\tilde{\boldsymbol{A}}^{\mathrm{W}}\cdot\boldsymbol{B}\,\mathrm{d}V,\qquad\text{where }\tilde{\boldsymbol{A}}^{\mathrm{W}}\equiv\boldsymbol{A}^{\mathrm{W}}-\boldsymbol{A}_0^{\mathrm{W}}. \tag{5.4}$$

Using the expression (4.11) for $\boldsymbol{A}^{\mathrm{W}}$ in proposition 1, we have

$$\tilde{\boldsymbol{A}}^{\mathrm{W}}\cdot\boldsymbol{B}=B_x\partial_yP-B_y\partial_xP+B_wT=-2\,\mathrm{Im}(\mathcal{B}\partial_zP)+B_wT, \tag{5.5}$$

where $\mathcal{B}\equiv B_x+\mathrm{i}B_y$ and P and T are real-valued flux functions.

On each $\mathcal{S}_w$, explicit expressions for P and T can be obtained by inverting the Poisson's equations (4.12) and (4.13) in terms of the (generalized) Green's function G_{p}, (2.23), i.e.

$$P(z,w)=-\int_{\mathcal{S}_w}B_w(z')\,G_{\mathrm{p}}(z,z')\,\mathrm{d}A_{z'}, \tag{5.6}$$

$$T(z,w)=-\int_{\mathcal{S}_w}J_w(z')\,G_{\mathrm{p}}(z,z')\,\mathrm{d}A_{z'}, \tag{5.7}$$

where $J_w=2\,\mathrm{Im}(\partial_z\mathcal{B})$ and the w-dependence of z is suppressed. Substituting (5.6) and (5.7) into (5.5) gives, noting that each $\mathcal{S}_w$-integral is performed with respect to z',

$$\begin{aligned}\tilde{\boldsymbol{A}}^{\mathrm{W}}\cdot\boldsymbol{B}&\\&=2\,\mathrm{Im}\int_{\mathcal{S}_w}\mathcal{B}(z)B_w(z')\partial_z\big[G_{\mathrm{p}}(z,z')\big]\,\mathrm{d}A_{z'}-2\int_{\mathcal{S}_w}B_w(z)\,\mathrm{Im}\big[\partial_{z'}\mathcal{B}(z')\big]\,G_{\mathrm{p}}(z,z')\,\mathrm{d}A_{z'} &(5.8)\\&=2\,\mathrm{Im}\int_{\mathcal{S}_w}\Big(B_w(z')\mathcal{B}(z)\partial_z\big[G_{\mathrm{p}}(z,z')\big]+B_w(z)\mathcal{B}(z')\partial_{z'}\big[G_{\mathrm{p}}(z,z')\big]\Big)\,\mathrm{d}A_{z'}\,, &(5.9)\end{aligned}$$

where we used integration by parts and that the boundary integral vanishes due to periodicity.

To proceed, we first assume $B_w\neq 0$. A complexified version of (5.2) is given by

$$\frac{\mathrm{d}z}{\mathrm{d}w}=\frac{\mathcal{B}[z(w)]}{B_w[z(w)]}, \tag{5.10}$$

and substituting it into (5.9) gives

$$\begin{aligned}\tilde{\boldsymbol{A}}^{\mathrm{W}}\cdot\boldsymbol{B}&=2\int_{\mathcal{S}_w}B_w(z')B_w(z)\,\mathrm{Im}\left(\frac{\mathrm{d}z}{\mathrm{d}w}\partial_z\big[G_{\mathrm{p}}(z,z')\big]+\frac{\mathrm{d}z'}{\mathrm{d}w}\partial_{z'}\big[G_{\mathrm{p}}(z,z')\big]\right)\mathrm{d}A_{z'} &(5.11)\\&=2\int_{\mathcal{S}_w}B_w(z)B_w(z')\,\mathrm{Im}\left[\frac{\mathrm{d}(z-z')}{\mathrm{d}w}\partial_zG_{\mathrm{p}}(z,z')\right]\mathrm{d}A_{z'}\,. &(5.12)\end{aligned}$$

In the last equality, we used the fact that $\partial_{z'}G_{\mathrm{p}}(z,z')=-\partial_zG_{\mathrm{p}}(z,z')$.

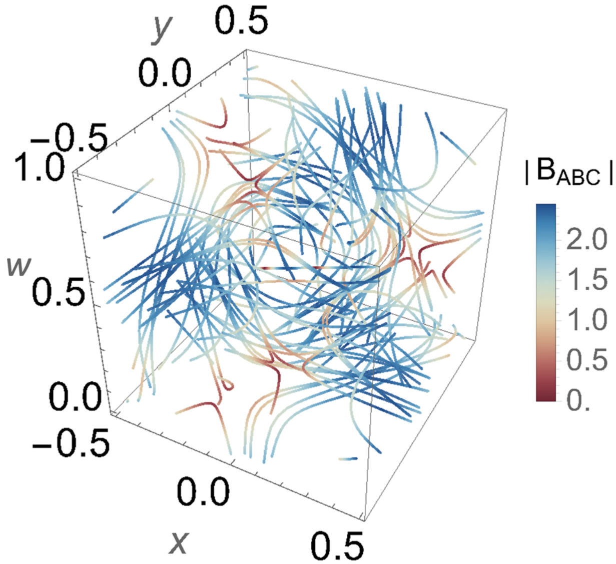

Figure 8. $\boldsymbol{B}$-lines of $\boldsymbol{B}_{\mathrm{ABC}}$ with $A=B=C=1$, coloured by the magnitude of field strength.

Recall that the pairwise periodic winding rate ω_{p} for two w-parameterized curves γ, γ', respectively, through z, z' (seen as projection on $\mathcal{S}$) is given by (2.27) as

$$\omega_{\mathrm{p}}(\gamma,\gamma') = 4\pi \,\mathrm{Im}\left[\frac{\mathrm{d}(z-z')}{\mathrm{d}w}\partial_z G_{\mathrm{p}}(z,z')\right]. \tag{5.13}$$

Comparing with (5.12) we have

$$\tilde{\boldsymbol{A}}^{\mathrm{W}}\cdot\boldsymbol{B} = \frac{1}{2\pi}\int_{\mathcal{S}_w}\omega_{\mathrm{p}}(\gamma,\gamma')B_w(z)B_w(z')\,\mathrm{d}A_{z'}\,. \tag{5.14}$$

In the case when $B_w=0$, the integrand of (5.14) vanishes identically, which can be used to *define* the excluded points. We now obtain (5.3) by integrating (5.12) over $V_{\mathrm{p}}=\mathcal{S}\times[0,1]$. ■

The complex formulation allows the periodic winding helicity to be more easily computed. Note that (5.3) would reduce to the Cartesian results (1.8) if ω_{p} was replaced with ω_{E}, noting that $\mathrm{d}A_z$ is the complex equivalent of $\mathrm{d}A$. We remark that results analogous to theorem 1 have been proved in non-periodic (or Euclidean) domains [9] and spherical domains [15].

(b) Example: winding helicity density of the ABC magnetic field

The Arnold–Beltrami–Childress (ABC) magnetic field [35] $\boldsymbol{B}_{\mathrm{ABC}}(\boldsymbol{x})$ is defined in V_{p} as

$$\boldsymbol{B}_{\mathrm{ABC}}(\boldsymbol{x}) = (A\sin\tilde{w} + C\cos\tilde{y})\hat{\boldsymbol{e}}_x + (B\sin\tilde{x} + A\cos\tilde{w})\hat{\boldsymbol{e}}_y + (C\sin\tilde{y} + B\cos\tilde{x})\hat{\boldsymbol{e}}_w, \tag{5.15}$$

where $\tilde{\boldsymbol{x}}=2\pi\boldsymbol{x}$ and A, B, C are fixed constants. Note that $\boldsymbol{B}_{\mathrm{ABC}}$ is periodic in all x, y and w directions with vanishing harmonic fluxes, $(\boldsymbol{B}_{\mathrm{ABC}})_0=\boldsymbol{0}$. For reference, figure 8 shows a three-dimensional streamline plot of $\boldsymbol{B}_{\mathrm{ABC}}$ with $A=B=C=1$, which will be used later. To illustrate the effects of harmonic fluxes, we add a constant harmonic field $\boldsymbol{B}_{\mathrm{H}}$ to $\boldsymbol{B}_{\mathrm{ABC}}$, i.e. we instead consider

$$\boldsymbol{B} = \boldsymbol{B}_{\mathrm{ABC}} + \boldsymbol{B}_{\mathrm{H}}. \tag{5.16}$$

Since the winding helicity $H^{\mathrm{W}}(\boldsymbol{B})$ is a single number for the entire field, we instead consider the spatial distribution of the integrand of (5.3) at some height w (up to a factor), i.e. the *winding*

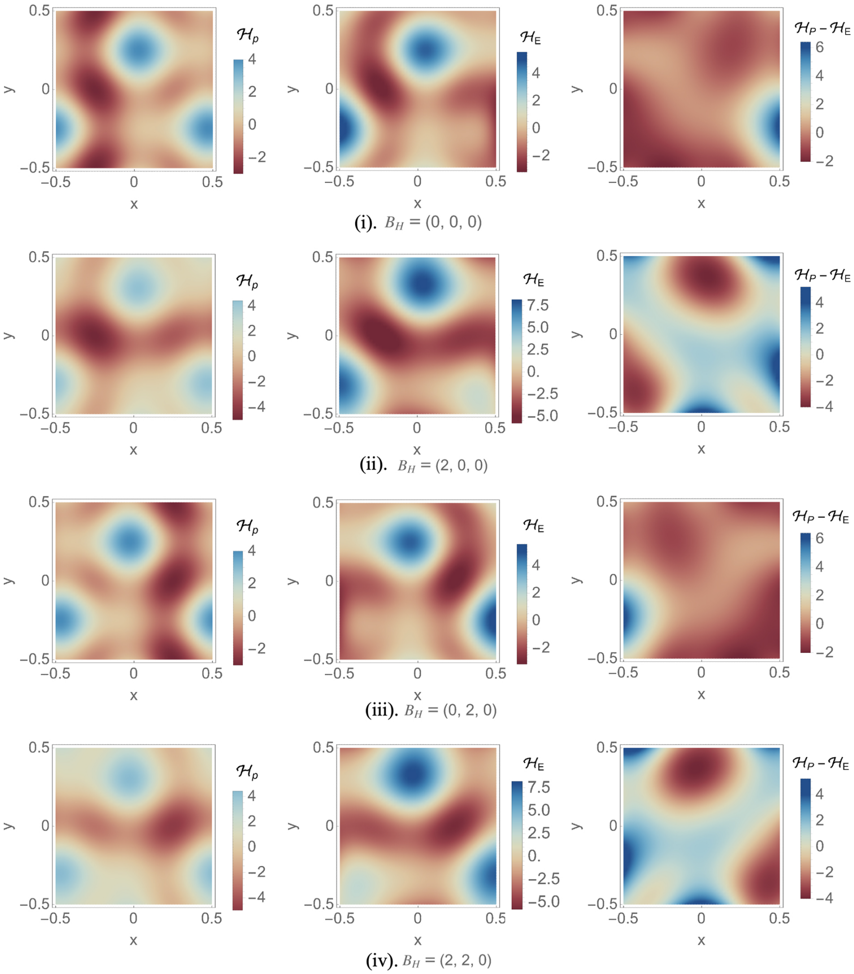

Figure 9. Spatial distributions of periodic winding helicity density $\mathcal{H}_\mathrm{p}$, (5.17) and its Euclidean version $\mathcal{H}_\mathrm{E}$, of $\boldsymbol{B} = \boldsymbol{B}_{\mathrm{ABC}} + \boldsymbol{B}_\mathrm{H}$, as well as their differences, for four choices of $\boldsymbol{B}_\mathrm{H}$. The same colour scales are used in the first two panels in each row (with the same $\boldsymbol{B}_\mathrm{H}$).

helicity density $\mathcal{H}_\mathrm{p}(z, w; \boldsymbol{B})$, defined by

$$\mathcal{H}_\mathrm{p}(z, w; \boldsymbol{B}) = \int_{\mathcal{S}_w} \omega_\mathrm{p}(\gamma, \gamma')B_w(z)B_w(z')\,\mathrm{d}A_{z'}. \tag{5.17}$$

Results of $\mathcal{H}_\mathrm{p}$ at $w = 0.5$ are plotted in figure 9, as well as its Cartesian analogue $\mathcal{H}_\mathrm{E}$ (replacing ω_p with ω_E and V_p with V_E in (5.17)) and their differences. Note that the computation of $\mathcal{H}_\mathrm{E}$ assumes that the $|\boldsymbol{B}| \to 0$ outside $\mathcal{S}$, also known as 'zero padding'.

For the same choice of $\boldsymbol{B}_\mathrm{H}$ (in each row), we typically have $|\mathcal{H}_\mathrm{p}| < |\mathcal{H}_\mathrm{E}|$ whereas the spatial distributions of $\mathcal{H}_\mathrm{p}$ display more periodicity (likely inherited from the domain). It is necessary to employ the correct expression as it would be difficult to quantify the differences that would arise.

6. Properties of winding helicity in periodic domains

As outlined in Berger [19], any meaningful definition of helicity $H(\boldsymbol{B})$ in the periodic domain $V_\mathrm{p} = \mathbb{T}^2 \times [0, 1]$ should satisfy the following properties:

(P1) $H(\boldsymbol{B})$ must reduce to its non-periodic counterpart in the suitable limits;

(P2) $H(\boldsymbol{B})$ is independent of translations and rotations of the representative of $\mathbb{T}^2$;
(P3) $H(\boldsymbol{B})$ is computable directly and unambiguously from $\boldsymbol{B}$;
(P4) $H(\boldsymbol{B})$ is conserved in ideal MHD flows;
(P5) $H(\boldsymbol{B})$ can be topologically interpreted as winding of $\boldsymbol{B}$-lines.

As discussed in §5, periodic winding helicity $H^{\mathrm{W}}(\boldsymbol{B})$ satisfies (P1)–(P3) and (P5), and (P4) will shortly be proved in §6a. We proceed in §6b to study how $H^{\mathrm{W}}(\boldsymbol{B})$ relates to helicity obtained in periodic domains from Fourier series [19,36,37]. Finally, in §6c, we discuss the geometrical implications of gauge transformations with respect to the winding gauge $\boldsymbol{A}^{\mathrm{W}}$.

(a) Time conservation in ideal MHD flows

To show (P4), we need to include time evolution and introduce a flow velocity $\boldsymbol{u}$ (with the required periodicity; same below for other variables). In ideal MHD flows, $\boldsymbol{B}$ and $\boldsymbol{u}$ are related via the *induction equation* [38] as

$$\frac{\partial \boldsymbol{B}}{\partial t} = \nabla \times (\boldsymbol{u} \times \boldsymbol{B}). \tag{6.1}$$

Assuming $\Phi = 0$, there exists some vector potential $\boldsymbol{A}$ such that $\boldsymbol{B} = \nabla \times \boldsymbol{A}$ and

$$\frac{\partial \boldsymbol{A}}{\partial t} = \boldsymbol{u} \times \boldsymbol{B} + \nabla \chi + \left(\frac{\partial \boldsymbol{A}}{\partial t}\right)_0, \tag{6.2}$$

accounting for possible gauge transformations (4.21) with χ any scalar field. Hence, we have:

Proposition 2 (P4). *Periodic winding helicity $H^{\mathrm{W}}(\boldsymbol{B})$ in V_{p} is conserved under ideal MHD evolution, given that on ∂V_{p} either (i) $\boldsymbol{B} \cdot \hat{\boldsymbol{e}}_w = \boldsymbol{u} \cdot \hat{\boldsymbol{e}}_w = 0$ or (ii) $\boldsymbol{B} \cdot \hat{\boldsymbol{e}}_w \neq 0$, $\boldsymbol{u} = \boldsymbol{0}$.*

Proof. Recall from (5.4) that for $\tilde{\boldsymbol{A}}^{\mathrm{W}} \equiv \boldsymbol{A}^{\mathrm{W}} - \boldsymbol{A}_0^{\mathrm{W}}$ we have $H^{\mathrm{W}}(\boldsymbol{B}) = \int_{V_{\mathrm{p}}} \tilde{\boldsymbol{A}}^{\mathrm{W}} \cdot \boldsymbol{B} \, \mathrm{d}V$. Since V_{p} is fixed, it follows that

$$\begin{aligned}
\frac{\mathrm{d}H^{\mathrm{W}}}{\mathrm{d}t} &= \int_{V_{\mathrm{p}}} \frac{\partial}{\partial t}(\tilde{\boldsymbol{A}}^{\mathrm{W}} \cdot \boldsymbol{B}) \, \mathrm{d}V && (6.3)\\
&= \int_{V_{\mathrm{p}}} [\tilde{\boldsymbol{A}}^{\mathrm{W}} \cdot \nabla \times (\boldsymbol{u} \times \boldsymbol{B}) + \nabla \chi \cdot \boldsymbol{B}] \, \mathrm{d}V && (6.4)\\
&= \int_{\partial V_{\mathrm{p}}} [\chi(\boldsymbol{B} \cdot \hat{\boldsymbol{e}}_w) + (\tilde{\boldsymbol{A}}^{\mathrm{W}} \cdot \boldsymbol{B})(\boldsymbol{u} \cdot \hat{\boldsymbol{e}}_w) - (\tilde{\boldsymbol{A}}^{\mathrm{W}} \cdot \boldsymbol{u})(\boldsymbol{B} \cdot \hat{\boldsymbol{e}}_w)] \, \mathrm{d}A\,. && (6.5)
\end{aligned}$$

Note that, we substituted (6.1) and (6.2) in (6.4) and used $\nabla \cdot \boldsymbol{B} = 0$ and Stokes' theorem in the last equality. It is immediate that (i) implies that $\mathrm{d}H^{\mathrm{W}}/\mathrm{d}t = 0$. For (ii), applying $\nabla_S \cdot$ to (6.2) while using $\nabla_S \cdot \boldsymbol{A}^{\mathrm{W}} = 0$ gives

$$\Delta_S \chi = 0 \implies \chi = \chi(w). \tag{6.6}$$

Assuming that $\Phi \equiv \langle \hat{\boldsymbol{e}}_w, \boldsymbol{B} \rangle = 0$ for each $\mathcal{S}_w \equiv \mathbb{T}^2 \times \{w\}$, we have, on $\partial V = \mathcal{S}_0 \cup \mathcal{S}_1$,

$$\frac{\mathrm{d}H^{\mathrm{W}}}{\mathrm{d}t} = \chi(1) \langle \hat{\boldsymbol{e}}_w, \boldsymbol{B} \rangle_{\mathcal{S}_1} - \chi(0) \langle \hat{\boldsymbol{e}}_w, \boldsymbol{B} \rangle_{\mathcal{S}_0} = 0. \tag{6.7}$$

■

We remark that the above proof can be seen as a simplified version of the general definition of relative helicity in multiply connected domains given by MacTaggart & Valli [21] that satisfies (P1)–(P4). However, relative helicity is too general to have a topological interpretation. Interested readers are referred to Prior & Yeates [9] for similar discussions on the non-periodic case.

(b) Fourier approach

We proceed to show that helicity defined via Fourier series can be made equivalent to winding helicity $H^{\mathrm{W}}(\boldsymbol{B})$ under suitable conditions. Let $\boldsymbol{x}_S \equiv (x, y)$ and $\boldsymbol{k} \equiv (k_x, k_y) = 2\pi(n_x, n_y) \in 2\pi\mathbb{Z}^2$. Then, any periodic vector potential $\boldsymbol{A}$ can be Fourier expanded as

$$\boldsymbol{A}(\boldsymbol{x}_S, w) = \hat{\boldsymbol{A}}_0(w) + \sum_{\boldsymbol{k}\neq\boldsymbol{0}} \hat{\boldsymbol{A}}_{\boldsymbol{k}}(w)\mathrm{e}^{\boldsymbol{k}\cdot\boldsymbol{x}_S}, \tag{6.8}$$

where the Fourier coefficients $\hat{\boldsymbol{A}}_{\boldsymbol{k}}$ (including $\boldsymbol{k} = \boldsymbol{0}$) are given by

$$\hat{\boldsymbol{A}}_{\boldsymbol{k}}(w) = \int_{\mathcal{S}_w} \boldsymbol{A}(\boldsymbol{x}_S, w)\mathrm{e}^{-\boldsymbol{k}\cdot\boldsymbol{x}_S}\,\mathrm{d}^2\boldsymbol{x}. \tag{6.9}$$

Note that the zero-mode $\hat{\boldsymbol{A}}_0$ is precisely the harmonic flux $\boldsymbol{A}_0$ defined in (4.5), same for $\boldsymbol{B}_0$.

The smoothness of $\boldsymbol{B}$ allows term-by-term differentiation of (6.8), i.e. $\boldsymbol{B} = \nabla \times \boldsymbol{A}$ and

$$\boldsymbol{B}(\boldsymbol{x}_S, w) = \underbrace{\nabla \times \hat{\boldsymbol{A}}_0(w)}_{\equiv\hat{\boldsymbol{B}}_0(w)} + \sum_{\boldsymbol{k}\neq\boldsymbol{0}} \underbrace{\left(\boldsymbol{k} \times \hat{\boldsymbol{A}}_{\boldsymbol{k}} + \hat{\boldsymbol{e}}_w \times \frac{\partial \hat{\boldsymbol{A}}_{\boldsymbol{k}}}{\partial w}\right)}_{\equiv\hat{\boldsymbol{B}}_{\boldsymbol{k}}(w)}\mathrm{e}^{\boldsymbol{k}\cdot\boldsymbol{x}_S}. \tag{6.10}$$

For each $\boldsymbol{k} \neq \boldsymbol{0}$, define a right-handed orthonormal wave-vector basis $\{\hat{\boldsymbol{e}}_w, \hat{\boldsymbol{e}}_{\boldsymbol{k}\parallel}, \hat{\boldsymbol{e}}_{\boldsymbol{k}\perp}\}$ where

$$\hat{\boldsymbol{e}}_{\boldsymbol{k}\parallel} \equiv \boldsymbol{k}/k = \hat{\boldsymbol{k}}, \qquad \hat{\boldsymbol{e}}_{\boldsymbol{k}\perp} \equiv \hat{\boldsymbol{e}}_w \times \hat{\boldsymbol{e}}_{\boldsymbol{k}\parallel}, \tag{6.11}$$

and $k = |\boldsymbol{k}|$, so that in this basis the Fourier coefficients of $\boldsymbol{A}$ and $\boldsymbol{B}$ are related via

$$\hat{B}_{\boldsymbol{k},w} = \mathrm{i}k\hat{A}_{\boldsymbol{k}\perp}, \quad \hat{B}_{\boldsymbol{k}\perp} = -\mathrm{i}k\hat{A}_{\boldsymbol{k},w} + \frac{\partial \hat{A}_{\boldsymbol{k}\parallel}}{\partial w}. \tag{6.12}$$

Note that

$$\hat{\boldsymbol{e}}_w \cdot \nabla \times \boldsymbol{B} = \sum_{\boldsymbol{k}\neq\boldsymbol{0}} \mathrm{i}k\hat{B}_{\boldsymbol{k}\perp}\mathrm{e}^{\boldsymbol{k}\cdot\boldsymbol{x}_S} = \sum_{\boldsymbol{k}\neq\boldsymbol{0}} \left(k^2\hat{\boldsymbol{A}}_{\boldsymbol{k},w} + \mathrm{i}k\frac{\partial \hat{A}_{\boldsymbol{k}\parallel}}{\partial w}\right)\mathrm{e}^{\boldsymbol{k}\cdot\boldsymbol{x}_S}, \tag{6.13}$$

and

$$\hat{\boldsymbol{e}}_w \cdot \boldsymbol{B} = \sum_{\boldsymbol{k}\neq\boldsymbol{0}} \hat{B}_{\boldsymbol{k},w}\mathrm{e}^{\boldsymbol{k}\cdot\boldsymbol{x}_S} = \sum_{\boldsymbol{k}\neq\boldsymbol{0}} (\mathrm{i}k\hat{\boldsymbol{A}}_{\boldsymbol{k}\perp})\mathrm{e}^{\boldsymbol{k}\cdot\boldsymbol{x}_S}. \tag{6.14}$$

Thus, if we define

$$P = \sum_{\boldsymbol{k}\neq\boldsymbol{0}} \hat{P}_{\boldsymbol{k}}\mathrm{e}^{\boldsymbol{k}\cdot\boldsymbol{x}_S} \equiv \sum_{\boldsymbol{k}\neq\boldsymbol{0}} (\hat{A}_{\boldsymbol{k}\perp}/k)\,\mathrm{e}^{\boldsymbol{k}\cdot\boldsymbol{x}_S}, \tag{6.15}$$

$$T = \sum_{\boldsymbol{k}\neq\boldsymbol{0}} \hat{T}_{\boldsymbol{k}}\mathrm{e}^{\boldsymbol{k}\cdot\boldsymbol{x}_S} \equiv \sum_{\boldsymbol{k}\neq\boldsymbol{0}} \hat{\boldsymbol{A}}_{\boldsymbol{k},w}\mathrm{e}^{\boldsymbol{k}\cdot\boldsymbol{x}_S}, \tag{6.16}$$

and *impose additionally* that for each $\boldsymbol{k} \neq \boldsymbol{0}$ that

$$\hat{\boldsymbol{A}}_{\boldsymbol{k}\parallel} = 0 \iff \nabla_S \cdot \boldsymbol{A} = 0, \tag{6.17}$$

and the global condition (4.14) for the zero-mode $\hat{\boldsymbol{A}}_0$, namely

$$\int_{V_{\mathrm{p}}} \hat{\boldsymbol{A}}_0 \cdot \nabla \times \hat{\boldsymbol{A}}_0\,\mathrm{d}V = \int_{V_{\mathrm{p}}} \hat{\boldsymbol{A}}_0 \cdot \hat{\boldsymbol{B}}_0\,\mathrm{d}V = 0, \tag{6.18}$$

we obtain precisely the winding gauge $\boldsymbol{A}^{\mathrm{W}}$ in proposition 1. This shows the necessity of the two extra constraints (6.17) and (6.18) for helicity to have a topological, winding-based interpretation, in addition to the usual Hodge decomposition[1].

[1]Note that Glasser [39] proved that the periodic Green's functions (2.23) can be derived from Fourier series.

(c) Gauge transformations

To further argue for the canonical status of the winding gauge $\boldsymbol{A}^{\mathrm{W}}$, we exhibit the geometrical significance of gauge transformations to the winding helicity $H^{\mathrm{W}}(\boldsymbol{B})$. In periodic domains V_{p}, we established in §4 that any admissible vector potential $\boldsymbol{A}$ is necessarily of the following form,

$$\boldsymbol{A} = \boldsymbol{A}^{\mathrm{W}} + \nabla\xi + \boldsymbol{G}_0, \tag{6.19}$$

for some function ξ and (horizontal) vector $\boldsymbol{G}_0$, from which helicity $H(\boldsymbol{B})$ can be written as

$$H(\boldsymbol{B}) = H^{\mathrm{W}}(\boldsymbol{B}) + \Delta H(\boldsymbol{B}), \tag{6.20}$$

where

$$\Delta H(\boldsymbol{B}) \equiv \int_{V_{\mathrm{p}}} (\nabla\xi + \boldsymbol{G}_0)\cdot\boldsymbol{B}\,\mathrm{d}V \tag{6.21}$$

$$= \int_{V_{\mathrm{p}}} \nabla\cdot(\xi\boldsymbol{B})\,\mathrm{d}V + \boldsymbol{G}_0\cdot\int_0^1\left(\int_{\mathcal{S}_w}\boldsymbol{B}\,\mathrm{d}^2\boldsymbol{x}\right)\mathrm{d}w \tag{6.22}$$

$$= \underbrace{\left(\int_{\mathcal{S}_1} - \int_{\mathcal{S}_0}\right)\xi B_w\,\mathrm{d}^2\boldsymbol{x}}_{\equiv\Delta H_{\mathrm{L}}(\boldsymbol{B})} + \underbrace{\boldsymbol{G}_0\cdot\int_0^1 \boldsymbol{B}_0\,\mathrm{d}w}_{\equiv\Delta H_{\mathrm{G}}(\boldsymbol{B})}. \tag{6.23}$$

In (6.22), we used $\nabla\cdot\boldsymbol{B} = 0$ and in (6.23), the divergence theorem was applied for $\partial V_{\mathrm{p}} = \mathcal{S}_0 \cup \mathcal{S}_1$. Note that $\Delta H(\boldsymbol{B})$ originates from the differences between $\boldsymbol{A}$ and the winding gauge $\boldsymbol{A}^{\mathrm{W}}$.

The change $\Delta H_{\mathrm{G}}(\boldsymbol{B})$ arises from the non-balanced harmonic flux $\boldsymbol{G}_0$ and is *global* in nature. It can be interpreted as the 'self-helicity' of $\boldsymbol{G}_0$ with the field $\boldsymbol{B}$ [34], which cannot be associated with the winding of $\boldsymbol{B}$-lines but nonetheless changes $H(\boldsymbol{B})$.

By comparison, the change $\Delta H_{\mathrm{L}}(\boldsymbol{B})$ is generated *locally* by the action of the scalar field ξ. From earlier works [9,15], it corresponds to changes in the winding-measuring directions. To see this, consider assigning a fictitious winding rate $\omega_{\mathrm{f}}(z,w)$ to every point in V_{p}, so that the modified pairwise winding rate $\tilde{\omega}_{\mathrm{p}}(w;\gamma,\gamma')$ through curves $z=\gamma(w)$, $z'=\gamma'(w)$ at height w is given by:

$$\tilde{\omega}_{\mathrm{p}}(w;\gamma,\gamma') \equiv \omega_{\mathrm{p}}(w;\gamma,\gamma') + \omega_{\mathrm{f}}(w;\gamma) + \omega_{\mathrm{f}}(w;\gamma'). \tag{6.24}$$

Following theorem 1, the extra contribution to winding can be associated with $\Delta H_{\mathrm{L}}(\boldsymbol{B})$, i.e.

$$\Delta H_{\mathrm{L}}(\boldsymbol{B}) = \frac{1}{2\pi}\int_0^1\int_{\mathcal{S}_w}\int_{\mathcal{S}_w}[\omega_{\mathrm{f}}(w;\gamma) + \omega_{\mathrm{f}}(w;\gamma')]B_w(z)B_w(z')\,\mathrm{d}A_z\,\mathrm{d}A_{z'}\,\mathrm{d}w\,, \tag{6.25}$$

and the corresponding scalar field ξ is given by, for example,

$$\xi(z,w) = \frac{w}{2\pi}\int_0^1\int_{\mathcal{S}_{w'}}[\omega_{\mathrm{f}}(w';\gamma) + \omega_{\mathrm{f}}(w';\gamma')]B_{w'}(z')\,\mathrm{d}A_{z'}\,\mathrm{d}w'\,. \tag{6.26}$$

Conversely, (6.25) can be used to determine (though non-uniquely) the fictitious winding rate ω_{f}. In both cases, the winding gauge $\boldsymbol{A}^{\mathrm{W}}$ corresponds to the case with no (net) global and local fictitious rotation, although $\boldsymbol{A}^{\mathrm{W}}$ is not uniquely fixed (as long as it satisfies proposition 1).

7. Discussion

In this work, we proposed a winding measure for planar curves in periodic domains $\mathcal{S} = \mathbb{T}^2 = \mathbb{R}^2/\mathbb{Z}^2$, i.e. the periodic winding rate ω_{p}, (2.13). Such a geometrical quantity provides helicity with an intrinsic interpretation and has generalized the existing formalism of winding-based open-field helicity, as the third piece in our trilogy following Prior & Yeates [9] and Xiao *et al.* [15]. Helicity, as shown in Prior and MacTaggart [13], can be interpreted as the combination of the 'geometrical' winding and the 'physical' magnetic field strength, both of which have independent temporal evolutions and different effects on the system's energetics. This work has significantly expanded on the applicability of existing studies.

A topologically different case concerns the singly periodic domain $\mathcal{C} = \mathbb{R}^2/\mathbb{Z}$ which is homoeomorphic to a two-cylinder, non-compact and multiply connected. Analogous to §2, the corresponding winding rate ω_s of a curve $\gamma : [0,1] \to \mathcal{C} \setminus \{0\}$ about $z = 0$ should read as, in complex notations,

$$\omega_s(t;\gamma) \equiv \operatorname{Im}\left[\pi \cot(\pi z)\frac{dz}{dt}\right], \tag{7.1}$$

where $\cot(\pi z)$ has the pole expansion by Mittag–Leffler theorem [23] that is similar to (2.9):

$$\pi \cot(\pi z) = \frac{1}{z} + \sum_{n\in\mathbb{N}^*}\left(\frac{1}{z-n} + \frac{1}{z+n}\right). \tag{7.2}$$

Note also that $\pi \cot(\pi z)$ is the derivative of the Green's function for Laplacian (up to a factor), i.e.

$$G_s(z) = \frac{1}{2\pi}\log|\sin \pi z|, \quad \text{where} \quad 4\pi\partial_z G_s(z) = \pi\cot(\pi z), \tag{7.3}$$

so that this case can also be included in the general expression (2.27) in §2c.

Note that, assumption $\Phi \equiv \langle \hat{e}_w \cdot \boldsymbol{B}\rangle = 0$ is necessary for compatibility with Stokes' theorem, since $\mathcal{S}$ is compact, boundaryless and multiply connected. Attention should be drawn to another case where functions are defined on $\mathbb{R}^2$ and are doubly periodic, but the underlying domain is simply connected and non-compact, as considered by, e.g. Panagiotou [18] in the simulation of filamentary networks to minimize the effect of boundary conditions. While such a distinction is well known in Fourier analysis [40], it is less emphasized in physics, so a detailed revisit is necessary. In particular, the fact that $\Phi \neq 0$ in general would invalidate all proofs in this work, especially violating the required periodicity of ω_p. We conjecture that the appropriate winding rate of planar curves would be (2.13) but without the $-\pi\bar{z}$ term that arises from the compactness-enforcing term in (2.19), which would be interesting to explore in future works.

Data accessibility. This paper has no additional data.

Declaration of AI use. We have not used AI-assisted technologies in creating this article.

Authors' contributions. D.X.: conceptualization, formal analysis, methodology, visualization, writing—original draft, writing—review & editing; C.B.P.: supervision, formal analysis, validation, writing—review & editing; A.R.Y.: supervision, validation, writing—review & editing.

All authors gave final approval for publication and agreed to be held accountable for the work performed therein.

Conflict of interest declaration. We declare we have no competing interests.

Funding. D.X. thanks parents for financial support during this work and is now supported by UK STFC grant ST/Y001672/1. A.R.Y. and C.B.P. were supported by UK STFC grant ST/W00108X/1.

Acknowledgements. We thank David MacTaggart and Adam Townsend for helpful discussions, as well as two anonymous referees for their constructive suggestions.

Appendix A. Winding for general curves

As mentioned in §1, Berger & Prior [11] proved that the Euclidean winding rate ω_E (2.2) can be used to define the winding number of curves that are not necessarily w-monotonic.

Let $\gamma, \gamma' : [0,1] \to \mathbb{C} \times [w_1, w_2]$ be smooth, non-intersecting space curves between horizontal planes $w = w_1$ and $w = w_2$ such that $\gamma(t) \neq \gamma'(t)$ for all $t \in [0,1]$. If γ, γ' are globally w-monotonic, then the Euclidean winding number is given in §2c as

$$L_E(\gamma,\gamma') = \frac{1}{2\pi}\int_{w_1}^{w_2} \omega_E[w;\gamma(w),\gamma(w)']dw. \tag{A 1}$$

In general, as shown in the example given in figure 1*b*, one can decompose γ, γ' into subcurves that are locally w-monotonic, say $\gamma = \cup_{i=1}^n \gamma_i$ and $\gamma' = \cup_{j=1}^m \gamma'_j$. Then, for each (i,j), there exists some (possibly empty) w-subinterval $[w_{ij}^{\min}, w_{ij}^{\max}]$ for which both γ_i and γ'_j are w-monotonic, so that the Euclidean winding number can be modified to

$$L_{\mathrm{E}}(\gamma,\gamma') = \sum_{i=1}^{n}\sum_{j=1}^{m} \frac{\sigma(\gamma_i)\sigma(\gamma'_j)}{2\pi} \int_{w_{ij}^{\min}}^{w_{ij}^{\max}} \omega_{\mathrm{E}}[w;\gamma_i(w),\gamma'_j(w)]\,\mathrm{d}w. \tag{A 2}$$

Here, to ensure the correct sign of crossings, we have defined an indicator function σ for the w-transversal direction as, e.g.

$$\sigma(\gamma_i) = \mathrm{sgn}\left(\left.\frac{\mathrm{d}\gamma_i}{\mathrm{d}t}\right|_{[w_1,w_2]} \right). \tag{A 3}$$

In the earlier derivation of winding helicity, e.g. (5.3) of theorem 1, the role of σ is automatically fulfilled by the sign of the normal magnetic field $B_w = \hat{\boldsymbol{e}}_w \cdot \boldsymbol{B}$.

If both γ and γ' are closed, then winding number (A 1) or (A 2) reduces to the usual Gauss linking integral and it is invariant under isotopy. If not, then it is also a topological invariant but now under end-vanishing isotopy, i.e. isotopy with endpoints of both curves fixed, although this does not hold in general for the Gauss linking integral.

In the periodic case, the same construction yields an analogous extension based on the periodic winding rate ω_{p}:

$$L_{\mathrm{p}}(\gamma,\gamma') = \sum_{i=1}^{n}\sum_{j=1}^{m} \frac{\sigma(\gamma_i)\sigma(\gamma'_j)}{2\pi} \int_{w_{ij}^{\min}}^{w_{ij}^{\max}} \omega_{\mathrm{p}}[w;\gamma_i(w),\gamma'_j(w)]\,\mathrm{d}w. \tag{A 4}$$

References

1. Woltjer L. 1958 A theorem on force-free magnetic fields. *Proc. Natl Acad. Sci. USA* **44**, 489–491. (doi:10.1073/pnas.44.6.489).
2. Moreau JJ. 1961 Constantes d'un îlot tourbillonnaire en fluide parfait barotrope. *C. r. hebd. séances Acad.*
3. Moffatt HK. 1969 The degree of knottedness of tangled vortex lines. *J. Fluid Mech.* **35**, 117–129. (doi:10.1017/S0022112069000991)
4. Arnold, VI. 2014 The asymptotic Hopf invariant and its applications. In *Vladimir I. Arnold - Collected Works: Hydrodynamics, Bifurcation Theory, and Algebraic Geometry* 1965–1972 (eds AB Givental, BA Khesin, AN Varchenko, VA Vassiliev, OY Viro), pp. 357–375. Berlin, Heidelberg, Germany: Springer. (doi:10.1007/978-3-642-31031-7_32)
5. Moffatt HK, Ricca RL. 1992 Helicity and the Călugăreanu invariant. *Proc. R. Soc. A* **439**, 411–4429. (doi:10.1098/rspa.1992.0159)
6. Cantarella J, DeTurck D, Gluck H. 2001 The Biot–Savart operator for application to knot theory, fluid dynamics, and plasma physics. *J. Math. Phys.* **42**, 876–905. (doi:10.1063/1.1329659)
7. Berger MA, Field GB. 1984 The topological properties of magnetic helicity. *J. Fluid Mech.* **147**, 133–148. (doi:10.1017/S0022112084002019)
8. Finn JH, Antonsen TMJ. 1985 Magnetic helicity: what is it and what is it good for. *Plasma Phys. Control. Fusion* **9**, 111–126.
9. Prior C, Yeates AR. 2014 On the helicity of open magnetic fields. *Astrophys. J.* **787**, 100. (doi:10.1088/0004-637X/787/2/100)
10. Démoulin P. 2007 Recent theoretical and observational developments in magnetic helicity studies. *Adv. Space Res.* **39**, 1674–1693. (doi:10.1016/j.asr.2006.12.037)
11. Berger MA, Prior C. 2006 The writhe of open and closed curves. *J. Phys. A: Math. Theor.* **39**, 8321. (doi:10.1088/0305-4470/39/26/005)
12. Berger MA. 1985 Topological invariants of field lines rooted to planes. *Geophys. Astrophys. Fluid Dyn.* **34**, 265–281. (doi:10.1080/03091928508245446)
13. Prior C, MacTaggart D. 2020 Magnetic winding: what is it and what is it good for? *Proc. R. Soc. A* **476**, 20200483 (doi:10.1098/rspa.2020.0483)

14. Prior C, Yeates AR. 2021 Intrinsic winding of braided vector fields in tubular subdomains. *J. Phys. A: Math. Theor.* **54**, 465701. (doi:10.1088/1751-8121/ac2ea3)
15. Xiao D, Prior CB, Yeates AR. 2023 Spherical winding and helicity. *J. Phys. A: Math. Theor.* **56**, 205201. (doi:0.1088/1751-8121/accc17)
16. Moffatt HK, Tsinober A. 1992 Helicity in laminar and turbulent flows. *Annu. Rev. Fluid Mech.* **24**, 281–312. (doi:10.1146/annurev.fl.24.010192.001433)
17. Pouquet A, Rosenberg D, Stawarz JE, Marino R. 2019 Helicity dynamics, inverse, and bidirectional cascades in fluid and magnetohydrodynamic turbulence: a brief review. *Earth Space Sci.* **6**, 351–369. (doi:0.1029/2018EA000432)
18. Panagiotou E. 2015 The linking number in systems with Periodic Boundary Conditions. *J. Comput. Phys.* **300**, 533–573. (doi:10.1016/j.jcp.2015.07.058)
19. Berger MA. 1996 Magnetic helicity in a periodic domain. *J. Geophys. Res.* **102**, 2637–2644. (doi:10.1029/96JA01896)
20. Pfefferlé D, Noakes L, Perrella D. 2021 Gauge freedom in magnetostatics and the effect on helicity in toroidal volumes. *J. Math. Phys.* **62**, 093505. (doi:10.1063/5.0038226)
21. MacTaggart D, Valli A. 2023 Relative magnetic helicity in multiply connected domains. *J. Phys. A: Math. Theor.* **56**, 435701. (doi:10.1088/1751-8121/acfd6c)
22. Berger MA. 1994 Minimum crossing numbers for 3-braids. *J. Phys. A: Math. Gen.* **27**, 6205–6213. (doi:10.1088/0305-4470/27/18/028)
23. Conway JB. 1978 *Functions of One Complex Variable*, vol. I, 1st edn. New York, NY: Springer.
24. Whittaker ET, Watson GN. 1996 *A Course of Modern Analysis*, 4th edn. Cambridge, UK: Cambridge University Press.
25. O'Neil K. 1989 On the Hamiltonian dynamics of vortex lattices. *J. Math. Phys.* **30**, 1373–1379. (doi:10.1063/1.528605)
26. Poulton CG, Botten LC, McPhedran RC, Movchan AB. 1999 Source-neutral Green's functions for periodic problems in electrostatics, and their equivalents in electromagnetism. *Proc. R. Soc. A* **455**, 1107–1123. (doi:10.1098/rspa.1999.0351)
27. Goncharov V, Gryanik V. 1986 Dynamics of solitary dissipative vortices: vortex lattices and their stability. *Zh. Eksp. Teor. Fiz.* **91**, 1653–1665.
28. Hensley D. 1994 The number of lattice points within a contour and visible from the origin. *Pac. J. Math.* **166**, 295–304.
29. Courant R, Hilbert D. 1989 *Methods of Mathematical Physics*. New York, NY: John Wiley & Sons, Ltd.
30. Lin CS, Wang CL. 2010 Elliptic functions, Green functions and the mean field equations on tori. *Ann. Math.* **172**, 911–954. (doi:10.4007/annals.2010.172.911)
31. Cantarella J, DeTurck D, Gluck H. 2002 Vector calculus and the topology of domains in 3-Space. *Am. Math. Mon.* **109**, 409–442. (doi:10.2307/2695643)
32. Hatcher A. 2009 *Algebraic Topology*. Cambridge University Press.
33. Reusken A. 2018 Stream function formulation of surface Stokes equations. *IMA J. Numer. Anal.* **40**, 109–139. (doi:10.1093/imanum/dry062)
34. Berger MA, Hornig G. 2018 A generalized poloidal–toroidal decomposition and an absolute measure of helicity. *J. Phys. A: Math. Theor.* **51**, 495501. (doi:10.1088/1751-8121/aaea88)
35. Dombre T, Frisch U, Greene JM, Hénon M, Mehr A, Soward AM. 1986 Chaotic streamlines in the ABC flows. *J. Fluid Mech.* **167**, 353–391. (doi:10.1017/S0022112086002859)
36. Cattaneo F, Bodo G, Tobias S. 2020 On magnetic helicity generation and transport in a nonlinear dynamo driven by a helical flow. *J. Plasma Phys.* **86**, 905860408. (doi:10.1017/S0022377820000690)
37. Yang KE, Wheatland MS, Gilchrist SA. 2020 Relative magnetic helicity based on a periodic potential field. *Astrophys. J.* **894**, 151. (doi:10.3847/1538-4357/ab8810)
38. Moffatt HK, Dormy E. 2019 *Self-Exciting fluid dynamos*. Cambridge, UK: Cambridge University Press.
39. Glasser M. 1974 The evaluation of lattice sums. III: Phase modulated sums. *J. Math. Phys.* **15**, 188–189. (doi:10.1063/1.1666619)
40. Körner TW. 1988 *Fourier Analysis*. Cambridge, UK: Cambridge University Press.